Cont #
N62269 80 019
10/5/83

NADC-82038-60

PRELIMINARY COPY

Materials Sciences Corporation

NOT ON CD-ROM

This is packing
sent on DTIC
Final Report
under
NADC-85013-60

COMPOSITE DEFECT SIGNIFICANCE

NADC
Tech. Info.

S. N. CHATTERJEE AND R. B. PIPES

19970606 011

DTIC QUALITY INSPECTED 2

Approved for Public Release; Distribution Unlimited

N62269-82-C-0705

Prepared for:
NAVAL AIR DEVELOPMENT CENTER
Warminster, PA

MSC TFR [illegible]
September, 1983

200074

DISCLAIMER NOTICE

THIS DOCUMENT IS BEST QUALITY AVAILABLE. THE COPY FURNISHED TO DTIC CONTAINED A SIGNIFICANT NUMBER OF PAGES WHICH DO NOT REPRODUCE LEGIBLY.

Materials Sciences Corporation

COMPOSITE DEFECT SIGNIFICANCE

Annual Technical Report
MSC TFR 1409/1109
September, 1983

Prepared by:
S. N. Chatterjee and R. B. Pipes

Prepared for:
Naval Air Development Center
Warminster, PA

Gwynedd Plaza II, Bethlehem Pike, Spring House, PA • 215-542-8400

REPORT DOCUMENTATION PAGE		READ INSTRUCTIONS BEFORE COMPLETING FORM
1. REPORT NUMBER NADC-82038-60	2. GOVT ACCESSION NO.	3. RECIPIENT'S CATALOG NUMBER
4. TITLE (and Subtitle) COMPOSITE DEFECT CRITICALITY		5. TYPE OF REPORT & PERIOD COVERED Technical Final Report 9/30/82 - 9/30/83
		6. PERFORMING ORG. REPORT NUMBER
7. AUTHOR(s) Sailendra N. Chatterjee and R. B. Pipes		8. CONTRACT OR GRANT NUMBER(s) N62269-82-C-0705
9. PERFORMING ORGANIZATION NAME AND ADDRESS Materials Sciences Corporation Gwynedd Plaza II, Bethlehem Pike Spring House, PA 19477		10. PROGRAM ELEMENT, PROJECT, TASK AREA & WORK UNIT NUMBERS
11. CONTROLLING OFFICE NAME AND ADDRESS W. R. Scott, Code 6063 Naval Air Development Center Warminster, PA 18974		12. REPORT DATE September 1983 13. NUMBER OF PAGES
14. MONITORING AGENCY NAME & ADDRESS(if different from Controlling Office)		15. SECURITY CLASS. (of this report) UNCLASSIFIED 15a. DECLASSIFICATION DOWNGRADING SCHEDULE

16. DISTRIBUTION STATEMENT (of this Report)

APPROVED FOR PUBLIC RELEASE; DISTRIBUTION UNLIMITED

17. DISTRIBUTION STATEMENT (of the abstract entered in Block 20, if different from Report)

18. SUPPLEMENTARY NOTES

19. KEY WORDS (Continue on reverse side if necessary and identify by block number)

Laminated Composites
Nondestructive Evaluation
Nondestructive Tests
Delaminations
Defect Criticality

20. ABSTRACT (Continue on reverse side if necessary and identify by block number)

This report outlines the various aspects of the program and describes work preformed to date on the following tasks:

(i) The preliminary master plan for effective utilization of NDE.

(ii) The symposium on NDE of Criticality of Defects in Laminated Composites.

(iii) Analytical Formulation of the problem of multiple

(20) ABSTRACT (cont'd.)

eliptic disbonds in Laminated Composites.

(iv) Experimental Study on Growth of Multiple disbonds under cyclic transverse shear and failure induced by static off-axis shear.

FOREWORD

This report summarizes the work performed for the Naval Air Development Center, Warminster, PA 18974 under the first year of contract N62269-82-C-0705, during the period September 30, 1982 to September 30, 1983.

The authors wish to express their sincere appreciation to Dr. W. R. Scott and Dr. B. W. Rosen for various suggestions and help during different stages of this work.

APPROVED:

Sailendra N. Chatterjee

Sailendra N. Chatterjee
Program Manager

TABLE OF CONTENTS

INTRODUCTION

The development of durable damage tolerant composite aircraft structures requires a sound understanding of the effects of defects. These effects are qualitatively, as well as quantitatively, different from the fracture mechanics of similar metallic structures. In recent years various studies have been conducted for assessing the effects of various kinds of defects in composite components. These studies have reached a point where an effort to integrate various advances is now desirable in order to define a reliable useful methodology for defect evaluations. This capability is needed for fleet life management and repair/replace maintenance decisions. To meet this objective the following major tasks were defined for the present program.

I. Formulation of a Master Plan - Elements of the methodology for generalized fracture mechanics and NDE of defect criticality in practical aircraft structures are to be studied. The study should address not only such technical issues as type of defects and method of evaluation, but also such management issues as technology transfer and training. Technology gaps in various areas should be identified and a program plan to fill these gaps should be drawn.

II. Perform analytical studies and experimental investigation for certain types of defects which are extremely critical like delaminations, bonded joints, etc.

This report summarizes the works performed to date in various areas during the first year of the present contract.

PRELIMINARY MASTER PLAN

An attempt is made in this plan to identify various aspects of the operational problem of nondestructive evaluation of criticality of defects in graphite epoxy composite components. Available nondestructive test methods and criticality assessment techniques are evaluated and a program plan describing the tasks, which should be performed for effective application of NDE to composite parts, is described. The plan was submitted in March, 1983, and was presented in the symposium on NDE of Criticality of Defects in Composite Laminates held in Valley Forge, PA, on May 23-24, 1983, organized by Materials Sciences Corporation under the sponsorship of Naval Air Development Center as a part of the present program. Based on the discussions and other presentations at the meeting as well as further review, the plan was revised and resubmitted (see ref. 1). Work on an expanded plan identifying a detailed program to fill up some of the technology gaps is being continued.

SYMPOSIUM ON NDE OF DEFECT CRITICALITY

As described in the last section a limited attendance symposium was conducted to discuss usefulness and shortcomings of the NDE methodologies, which can be currently used in practice, areas where further research and developmental work is needed as well as the present state of the art of inspection and repair technology of composite components. Vu-graphs of presentations and transcribed discussions are being compiled in the form of an informal symposium proceedings. This work will be completed by October, 1983. A discussion for some of the presentations is given next.

1. "Use of Thermography to Detect and Quantity Damage in Fiber Composite Laminates", by P. V. McLaughlin, Jr. Monitoring the surface temperature due to an externally applied thermal field by the use of an infrared camera is demonstrated to be a useful tool in locating and quantifying defects. From the point of view of practical application there are, however, some problem areas like heat generation and noise. Increased sensitivity of the monitoring instrument may be helpful to sort out some of the difficulties.

2. "Ultrasonic Correlation to Porosity in Graphite Epoxy Laminates", by R. Collins. This subject is of great importance, since quantifying porosity by NDE is a difficult task. Although the results indicate that some correlations can be established between porosity as determined from image analysis and the Db gain at which an indication fails to trigger the recorder amplitude gate, further work appears necessary before this can be used in routine applications.

3. "Hole Wear in Composites due to Bearing Loads", by R. Badaliance. Fastener hole wear damage due to fatigue loading is found to be a local one caused by matrix cracks and subsequent

pulverization of the material due to bearing loads. A semi-empirical correlation between strain energy density stored in an infinitesimal volume element at the location of maximum bearing pressure and constant amplitude hole wear lives is attempted. This relationship and Miner's rule are utilized to compare predicted spectrum lives with test data for different laminates under various environments. The approach appears to be useful as a design tool. However, its usefulness as a NDE technique is limited, since no correlation is attempted between extent of damage and residual life time.

4. "On the Role of Damage Tolerance Analysis in Nondestructive Evaluation of Composite Structures", by D. J. Wilkins. Application of semi-empirical growth laws and 3-D finite element analysis for calculation of energy release rates in predicting growth of a delamination under fatigue loading is illustrated. Advantages of fabric and 3-D reinforcements for increasing damage tolerance of composite structures are also pointed out.

5. "Ultrasonic Waves and Composite Material Testing", by W. Sachse. Use of ultrasonic attenuation and velocity measurements in detecting material inhomogeneities and flaws is examined. Further research is needed before these techniques can be used in practice.

6. "Computer Aided Ultrasonic Measurement of Tangential Flaw Boundary Growth in Composite Materials", by R. A. Blake, Jr. The procedure of obtaining digital ultrasonic C-Scans on a color graphic computer is described and its usefulness in monitoring growth of delaminations and other kinds of flaws is discussed. The technique of computer aided image enhancing appears attractive, but more work is needed for routine application. It will be of interest to compare such measurements with those from other techniques like penetrant enhanced X-ray radiography.

7. "Interlaminar Stress Field as Influenced by two interacting flaws", by A. S. D. Wang. Finite element calculation of stress fields near interacting intralaminar cracks and interlaminar de-

laminations and energy release rates at such crack and delamination fronts are reported. Correlation of predictions obtained from such analyses and test data appears necessary for demonstrating their usefulness.

8. "Repair Technology for Advanced Composites", by E. Rosenzweig. Currently used NDE procedures and repair techniques are discussed. It is reported that depot level inspections are being de-emphasized, placing more importance on on-site inspection. This might necessitate a re-examination of currently used NDE techniques.

9. "Presentation of a Preliminary Plan to fill the Technology Gaps", by S. N. Chatterjee. The preliminary plan discussed in the previous section is presented.

10. "Potential of Accoustic Emission Technique for Monitoring Damage During Quasi-static and Fatigue Loading" by J. Awerbuch. Use of this technique as a research tool is demonstrated. Its usefulness as a NDE technique for evaluating criticality of defects appears limited.

11. "Defect Enhanced Fatigue Failure in Graphite/Epoxy Composites", by R. J. Richards-Frandsen, et. al. Delamination induced failure is studied experimentally and a semi-empirical correlation is attempted. Use of more refined analytical procedures in calculation of stress intensity factors may yield better correlations.

12. "Effects of Porosity, Delamination and Low Velocity Impact Damage on the Compressive Behavior of Graphite/Epoxy Laminates", by R. L. Ramkumar. Test data and some analytical results for different types of defects are surveyed and their usefulness for design applications are pointed out. Severity of different kinds of defects is also discussed.

13. "Compressive Strength of Composite Laminates with Interlaminar Defects" by J. W. Gillespie, Jr. et. al. Growth of delaminations in presence of imperfections of wavy shape under compressive loads is studied.

14. "Damage Zone Development in Notched Graphite Epoxy Composites" by J. Slepetz. The complicated nature of damage growth in notched composites is discussed.

In addition to the presentations discussed above use of approximate methods of stress analysis were considered by D. Y. Konishi and L. W. Rehfield. Overviews of work sponsored by Air Force were presented by G. Sendeckyj, who described some attempts of using CAT-Scans for detection of defects. D. Mulville provided an overview of Navy sponsored works in different areas. From the presentations and discussions it appears that NDT methods and criticality assessment techniques (in many cases semi-empirical ones based on test data on similar materials) are available for a variety of defects. The problem of choosing the right tool or tools for effective utilization of NDE, however, requires further research and developmental work in this direction.

ANALYTICAL TASKS

Analytical tasks to be performed under the program are described below.

1. Stress analysis near multiple elliptic disbonds in a laminated plate and correlation with results from experimental tasks on growth of such delaminations under cyclic loading.
2. Analysis of delamination near ply drops.
3. An analysis of failure of bonded joints and correlation with test data from experimental program.
4. Comparison of results from two analyses of the delamination problem.
5. Demonstration of usefulness of analysis methods with application to a practical situation.

A method of analysis has been formulated for the multiple delamination problem. A cluster of delaminations are considered as shown in figure 1. Details of the analysis are given in appendix A-1. A computer program is being developed. Some progress has been made in the bonded joint analysis considering possible separation near the ends in peel mode but allowing for shear transfer through an interdigitated interface. Details will be reported in the next reporting period.

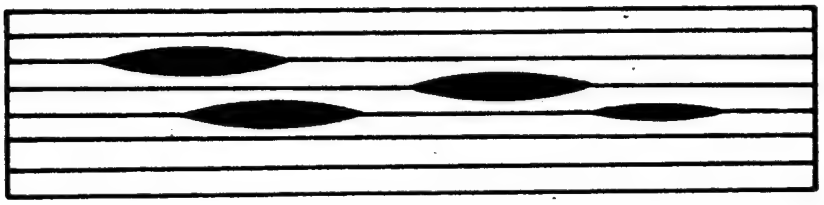

Section AA

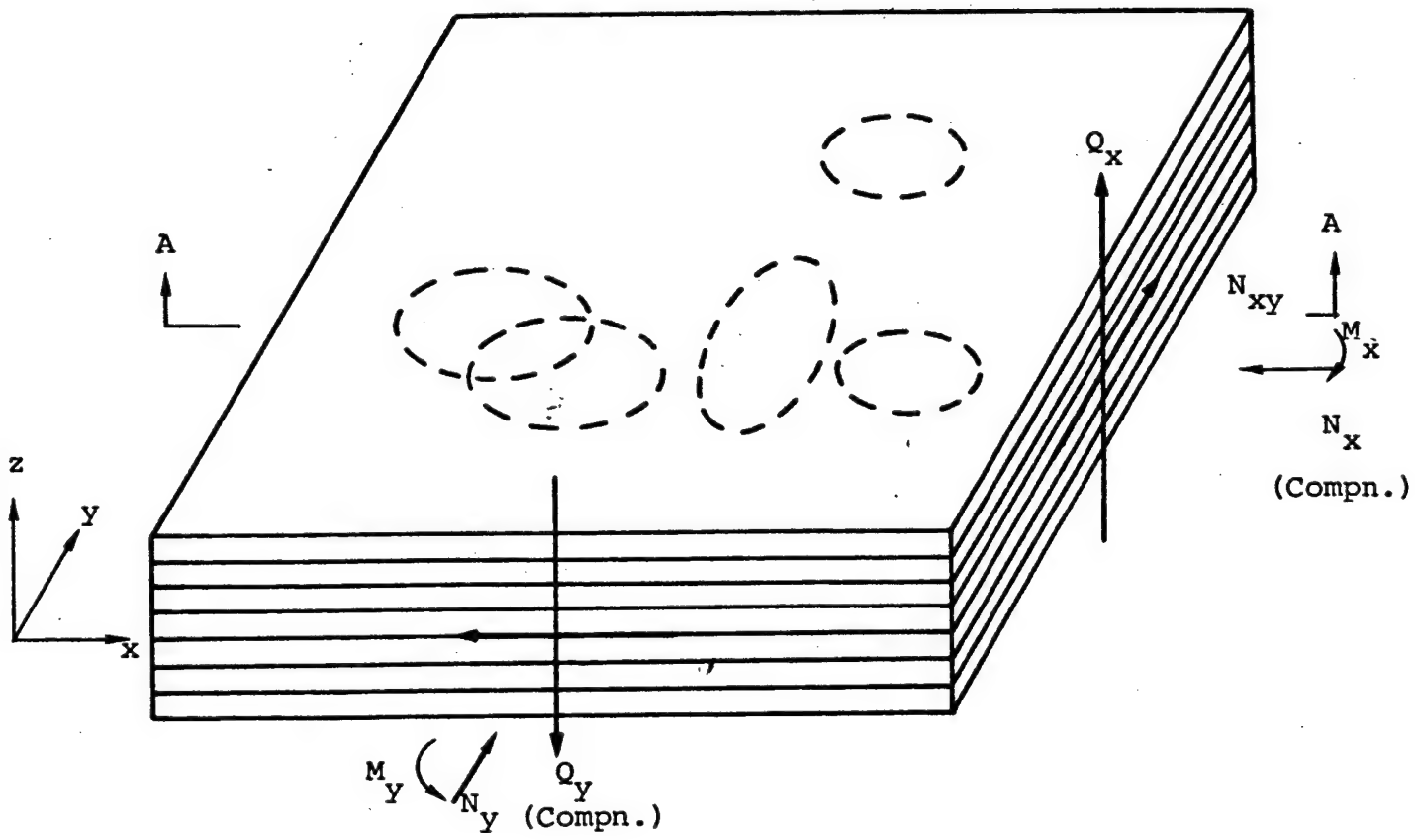

Figure 1. Delaminations in a Laminated Plate

EXPERIMENTAL PROGRAM

The experimental study has been separated into three test programs with five individually identifiable tasks, depicted in Table 1. Test series involving multiple delaminations in Mode II shear are similar to those conducted under previous programs, (ref. 2, 3) while the investigation of biaxial flaw criticality and the analysis of bonded composite structures with adhesive delaminations are new areas of interest.

TASK I. - MULTIPLE DELAMINATIONS IN MODE II SHEAR

The effects of multiple delaminations on Mode II dominated flaw growth are under investigation using flexural fatigue specimens in three-point bending. Experimental procedures have been developed in previous test programs investigating Mode II flaw growth for single elliptical delaminations (ref. 2, 3). The three-point bend test fixture employed is shown in Figure 2, where delaminations are implanted at equal distance from end support and center load on both the left and right halves of the test specimen.

A total of 30 specimens are being tested in three-point bending to examine the Mode II dominated response of delaminated plates. Twenty-four samples are under test in flexural fatigue and six specimens were failed in a static mode to provide baseline data. Table 2 describes the sample designations and test specimen configurations for Task 1.

Two elliptical debond geometries are investigated, $b/a = 1.0$ and 1.5, where the minor axis "a" is 1 inch, and normal to the longitudinal direction of the specimen. The circular debonds have been chosen for investigation for direct correlation with data generated previously for the single circular debond. Delaminations are implanted at the midsurface (Location 1) and at quarter-thickness in both the compressive (Location 2) and tensile regions (Location

Table 1

Program Outline

a) 3 Test Programs

Multiple Delaminations in Mode II Shear

Biaxial Testing

Bonded Composite Structures

b) 5 Identifiable Tasks

1) Multiple Delaminations

2) Off-axis Shear - Biaxial

3) Honeycomb Crossbeams - Biaxial

4) Bonded Joints with Defects

5) Bonded Joints without Defects

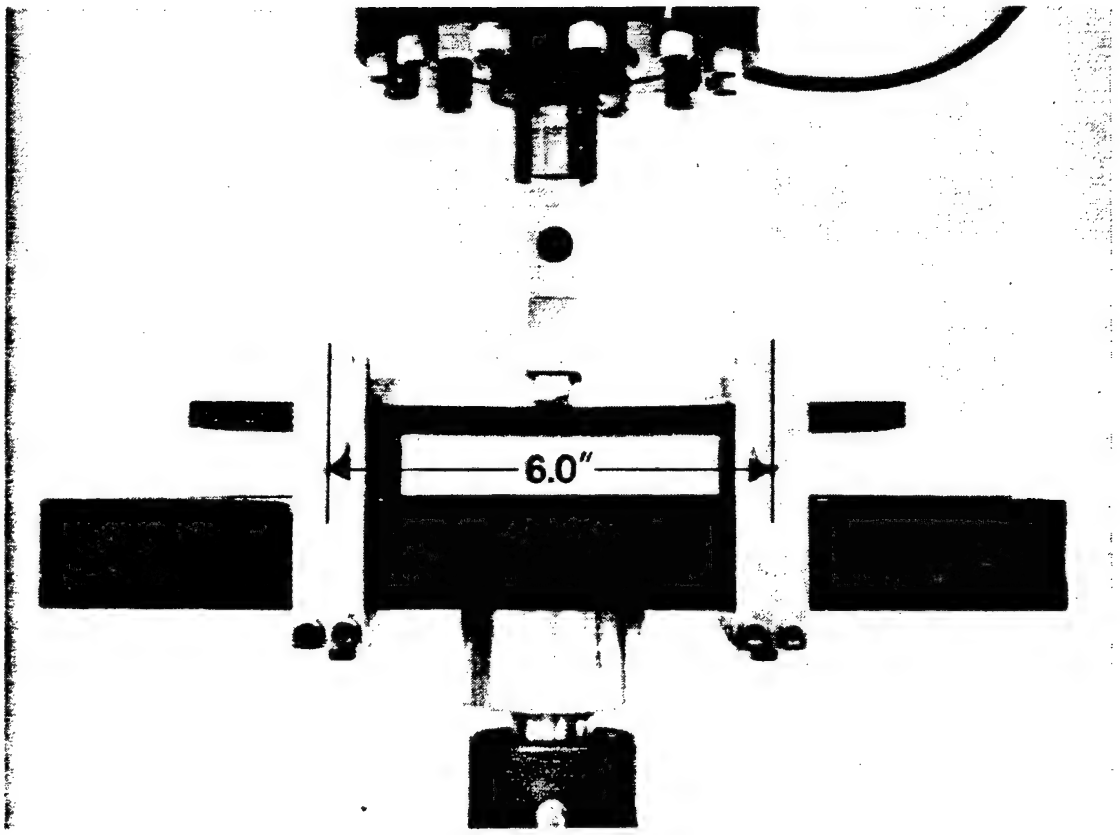

Figure 2. Thick beam in three-point bending

Table 2

Task 1

Laminate Stacking Sequences

A: $(0_8/+45_4/-45_4/0_6/+45_4/-45_4/0_2)_s$

B: $(0_4/\pm45_2/\mp45_2/0_4)_{2s}$

C: $(-45_4/+45_4/0_{10}/-45_4/+45_4/0_6)_s$

Sample Designations

Ex: 1.0-A 1
Task "1"
Defect Configuration "0", none
Laminate "A"
Sample "1"

1.2-B 3
Task "1"
Defect Configuration "2"
Laminate "B"
Sample "3"

Multiple Delamination Configurations

Configuration		Location*	
		Left	Right
1	b/a = 1.5	Location 1 Location 2	Location 1 Location 3
2	b/a = 1.0	Location 1 Location 2	Location 1 Location 3
3	b/a = 1.0 b/a = 1.5	Location 1 Location 2	Location 1 Location 3
4	b/a = 1.5	Location 2 Location 3	Location 2 Location 3

*Location 1: Debond at midsurface
Location 2: Debond at quarter-thickness in compression
Location 3: Debond at quarter-thickness in tension

3) of the flexure specimen. Fatigue tests are run at a single S-level of 0.5 and three replicates are being tested for each geometry.

Table 3 presents static test results for the no-defect configuration. These data were used to set the S-level for all subsequent fatigue tests.

For both the A and B laminates, the failure is initiated at the compressive surface. However, the fracture patterns of the two stacking sequences are different (see Figure 3). The B laminate, with $\pm 45_2$ plies, shows only a compressive failure of the outermost 0° plies. The A laminate, however, has both a compressive failure, as well as, considerable interply fracture between the $+ 45_4$ and $- 45_4$ lamina. In the B laminates $(\pm 45_2)_s$ sublaminate appears to have arrested this failure mode. Fractographic analysis of these failure surfaces remains to be performed in the second year. It should be pointed out that the failures are in flexural mode and not induced by flaw growth because of small delamination sizes. Flaw growths are noticed under cyclic loading as discussed in the following paragraph. Large size disbonds can initiate failure due to catastrophic flaw growth (ref. 4).

The fatigue program for Task 1 is progressing. All samples in both A and B geometries have been fabricated and C-scanned, and all of the A laminate specimens are being actively tested. Samples from geometry 1.1-An have been tested to failure, while sample sets 1.2, 1.3, and 1.4 are underway, all having undergone at least 100,000 cycles, with many exceeding 150,000 to date.

Ultrasonic C-scanning is being used to nondestructively monitor the growth of the delaminations during load cycling. In order to individually monitor the flaw growth of the disbonds implanted at the quarter-planes and the midsurface, four separate C-scans are necessary for 1.1, 1.2, and 1.3, specimens. These scans are designated as C, T, MC, and MT, for compressive quarter-plane, tensile quarter-plane, compressive-viewed midplane, and tensile-viewed midplane, respectively. Figure 4 describes the gating

Table 3

Task 1.0 Results

	Max Load (kg)	Thickness (mm)	Width (mm)
1.0-A 1	2800	8.9	76.6
1.0-A 2	2650	8.6	76.2
1.0-A 3	2900	9.0	76.0
Average	2783		
1.0-B 1	2950	9.0	76.3
1.0-B 2	2400	8.1	76.3
1.0-B 3	2700	8.7	76.7
Average	2683		

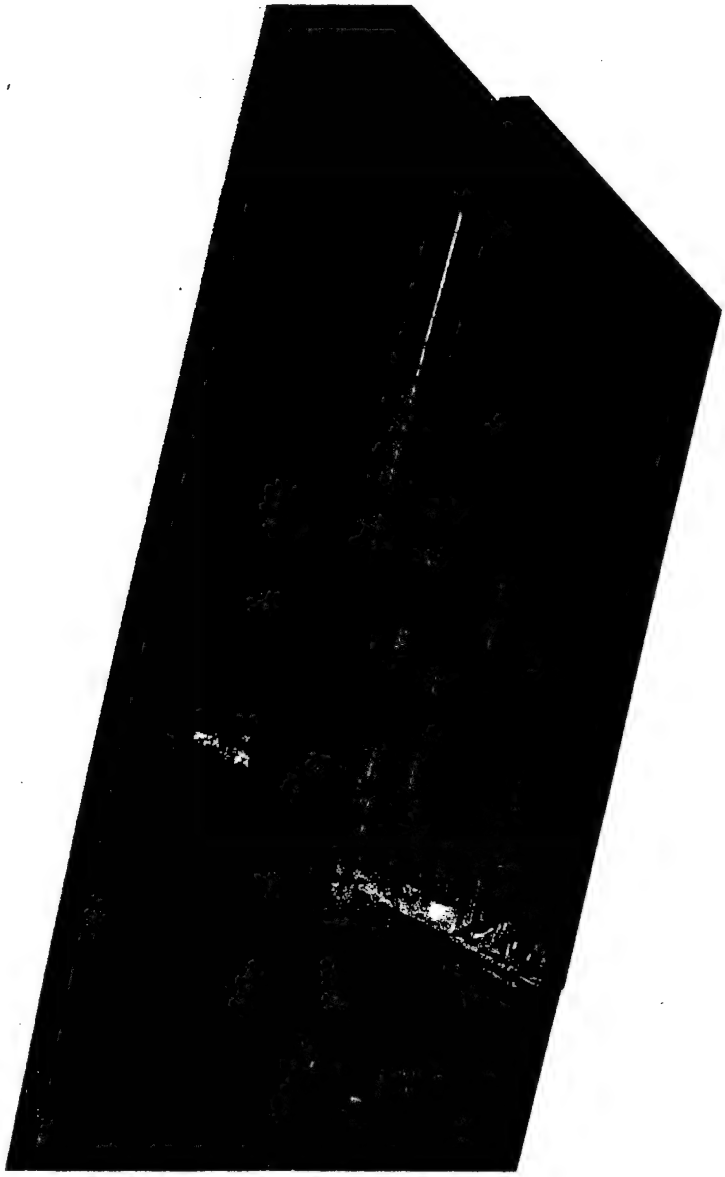

Figure 3 Task 1 Static Failures

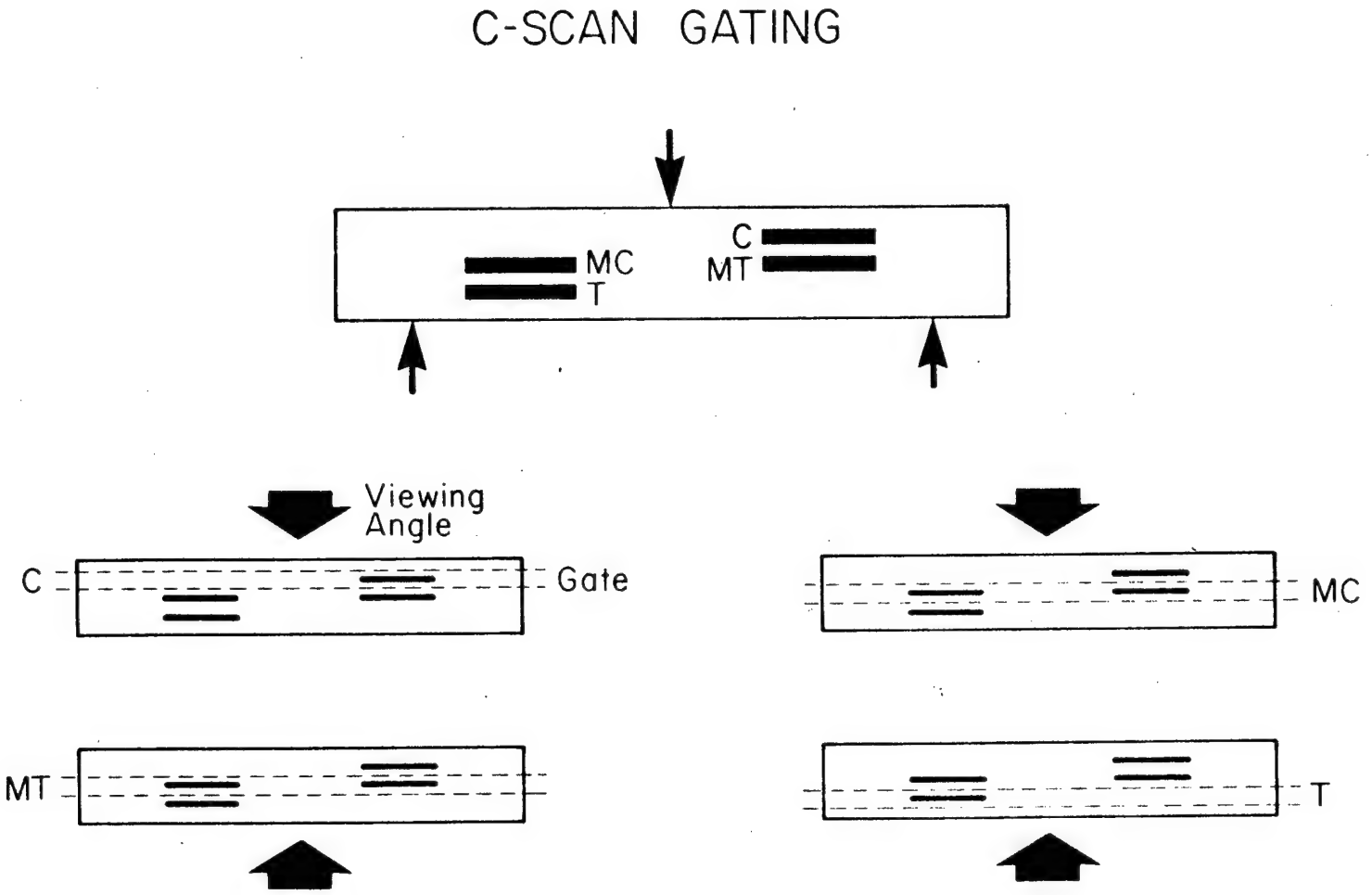

Figure 4 Gating Procedure

and viewing scheme employed to monitor the individual growth patterns of the delaminations. Since disbonds are implanted only at the quarter-planes for samples 1.4, only C and T scans are needed. A series of C-scans for one sample from 1.2, 1.3, and 1.4 configurations comprise Appendix A2.

In earlier static tests (see figure 28 in reference 4) it has been noted that interlaminar shear cracks "stepped up" through the 0^{o} plies in which they were implanted to run along a 0/45 interface. This, however, appeared to have occured after the disbonds have grown sufficiently large (elongated) in the original plane. In the current work, disbonds are implanted at the quarter-plane, which is a -45/0 interface for the A laminate. To examine the behavior of the crack front originating between -45/0 plies, a series of C-scans were done on specimen 1.4-A 2 after 110,000 cycles using a narrow gate focussed above, at, and below the implant. The sequence of five C-scans are presented as Figure 5. The ultrasonic images show that the delamination crack front does change laminate planes, to "step up", in this case to the +45/-45 interface, cutting through -45^{o} plies.

Flaw growth will be measured radially from the center of the implanted defects by either manual or computer-aided inspection techniques following completion of the test program. The radius, r, and angle, θ, measurements are expected to produce superior flaw characterization as compared to point measurements made along the axis of the beam as has been performed in previous studies.

TASK II. - BIAXIAL TESTING THROUGH OFF-AXIS SHEAR

A three point bend test using an off-axis laminate is being used to generate a biaxial state of interlaminar shear stress. The relative magnitude of these stresses is limited and dependent upon the material properties, layup, and the angle of orientation between the loading direction and principal material direction. The effects of bending-twisting coupling, however, are known to die out

Figure 5. Scans, Specimen 1.4-A2 Gated above, at and below

with increasing number of plies. The specimen geometry and test methodology are indentical to those employed in Task 1. The initial stacking sequence - laminate A - is a 15° rotated version of laminate B from Task 1, ie. $[+15_4/(+60/-30)_2]_{s4}$. Depending on results of this orientation, a second orientation will be defined, most likely either a +30° or +10° series. Table 4 shows the sample configurations.

In all, eighteen static and twelve fatigue specimens are to be tested in off-axis shear to examine biaxial loading response of graphite-epoxy laminates containing delaminations.

To date, static specimens from laminate "A" have been tested to failure, and the fatigue samples have been fabricated. Static test results are shown in Table 5.

The dominant failure mode for the static test specimens is intra-ply splitting of the surface plies on both the tensile and compressive sides. Figure 6 shows the common failure topography. The large magnitude of surface cracking provided many pathways for the water used as the couplant during ultrasonic inspection to enter the laminate and mask the interlaminar features. To circumvent this problem, the laminates were dipped in common paraffin wax to seal the surface cracks. The excess wax was scraped from the plates and the samples were subsequently scanned in the normal manner. A C-scan of a wax-sealed specimen is depicted in Figure 7, which shows no growth of disbonds has occured. It is expected that they will grow under cyclic loading.

TASK III. - BIAXIAL TESTING USING CROSS-BEAM HONEYCOMB SANDWICH SPECIMENS

A simple method to develop biaxial in-plane stress is to use a cross-beam specimen as shown in Figure 8. The material under test is bonded to one surface of a high density honeycomb core material, a stronger skin is then bonded to the opposing face, creating a sandwich structure in the form of a cross. The per-

Table 4

Task 2 - Off-axis Shear Specimen Configuration

Laminate A: $(+15_4/(+60/-30)_2)_{s4}$

Laminate B: $(+30_4/(+75/-15)_2)_{s4}$

Samples: 2.0-A 1,2,3
2.1-A 1,2,3

Defect Configurations:

0 - no defect

1 - circular, r = 1.8"

2 - elliptical, a = 1.7", b = 2.0"

Table 5

Static Test Results - Biaxial Thick Beams

	Max Load (kg)	Thickness (mm)	Width (mm)
2.0-A 1	1790	8.9	76.2
2.0-A 2	1800	8.7	76.4
2.0-A 3	1840	8.9	76.8
Average	1810		
2.1-A 1	1800	9.0	74.9
2.1-A 2	1825	9.1	76.7
2.1-A 3	1840	8.9	76.7
Average	1822		

Figure 6 Task 2 Static Failure of Off-axis Shear Specimens

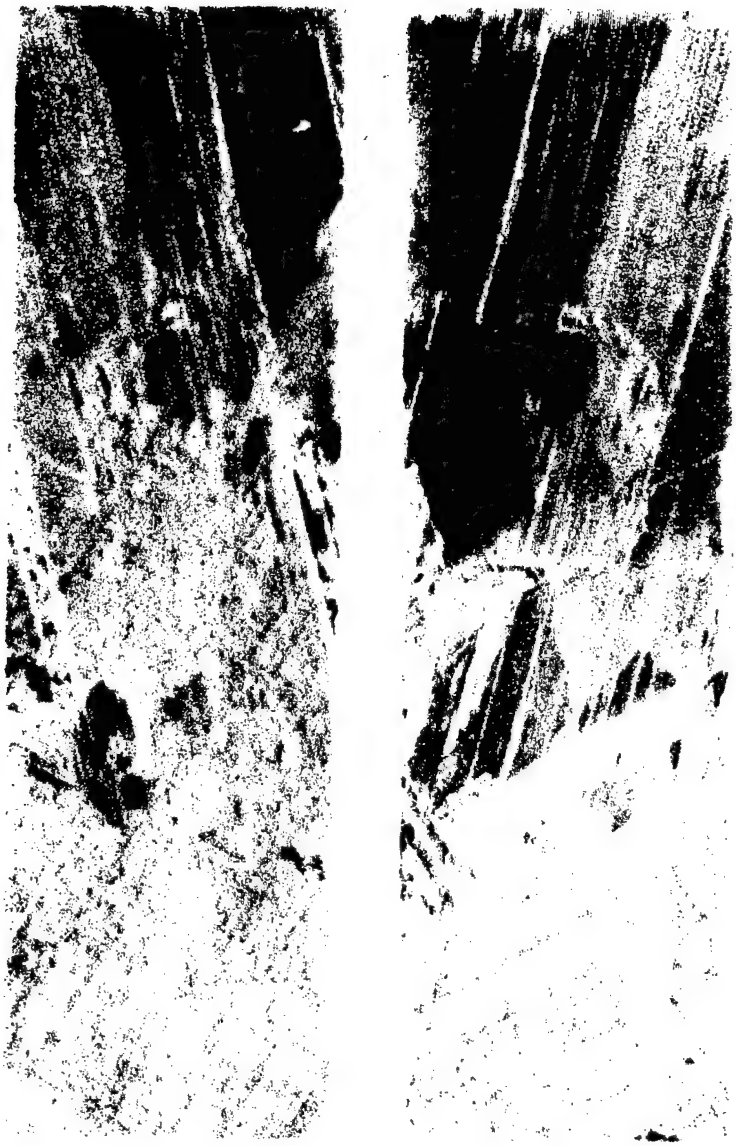

Figure 7. C-scan of Wax-sealed Off-axis Shear Specimens

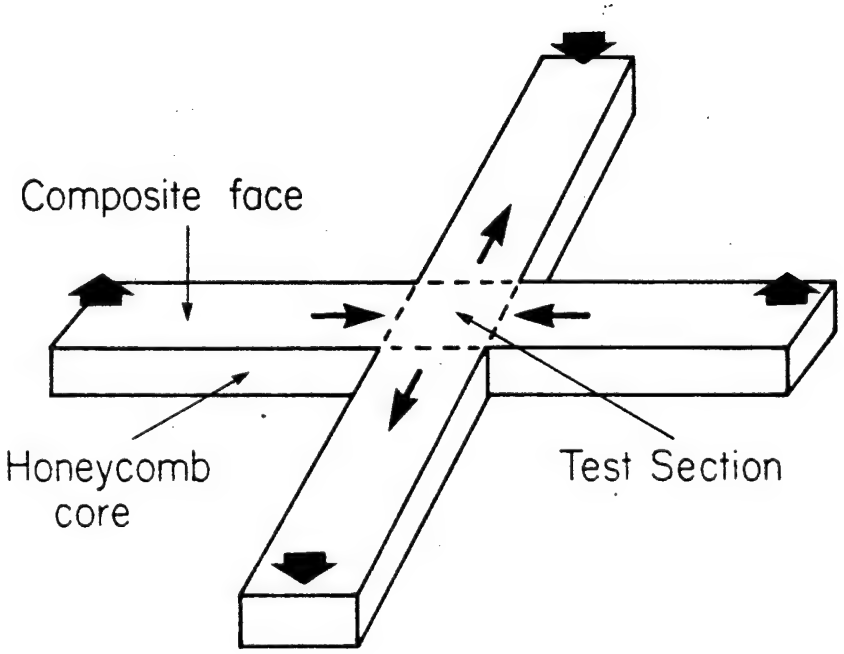

Figure 8. Cross sandwich beam test specimen

pendicular beams are then loaded in four point bending, in this case producing a tensile stress in one direction and a compressive component in the other.

A test program employing an eight-ply quasi-isotropic skin has been developed to verify the viability of this test method for study of delamination growth in biaxially loaded panels. A total of twelve specimens are to be tested as described in Table 6. Teflon disks of one inch diameter will be implanted for the six beams with delaminations.

To date, the test fixture has been designed and fabricated and some of the graphite-epoxy skins have been layed-up and cured. No complete specimens have been finished or tested.

TASK IV. - BONDED COMPOSITE STRUCTURES

The strength and delamination growth in bonded composite structures is under investigation utilizing the single lap joint test specimen geometry. The lap joint consists of two eight-ply quasi-isotropic adherends and American Cyanamid's FM300M adhesive used commonly on several aircraft structures. The test program includes tension-tension fatigue and static tests to address delamination growth and strength respectively.

A total of 27 specimens are to be tested in the bonded joint program, nine in static mode and 18 in tensile fatigue. Two teflon disbond geometries will be employed, as well as, a no-defect series. Figure 9 shows the delamination geometries to be tested.

A preliminary study was undertaken to determine the pristine joint strength as a function of bond length and to generate mechanical property data for the laminate. The initial set of specimens tested showed no sensitivity to bond length, even at the extremes of 10 mm to 100 mm. New adhesive was acquired to retest the bond strength; sample fabrication is continuing, including dessication of the graphite-epoxy laminates prior to bonding.

A few samples were bonded with Tedlar film implants to study

Table 6

Honeycomb Sandwich Specimens

	Fatigue ($s=0.5$)	Static
No Disbond	3	3
1" Disbond	3	3

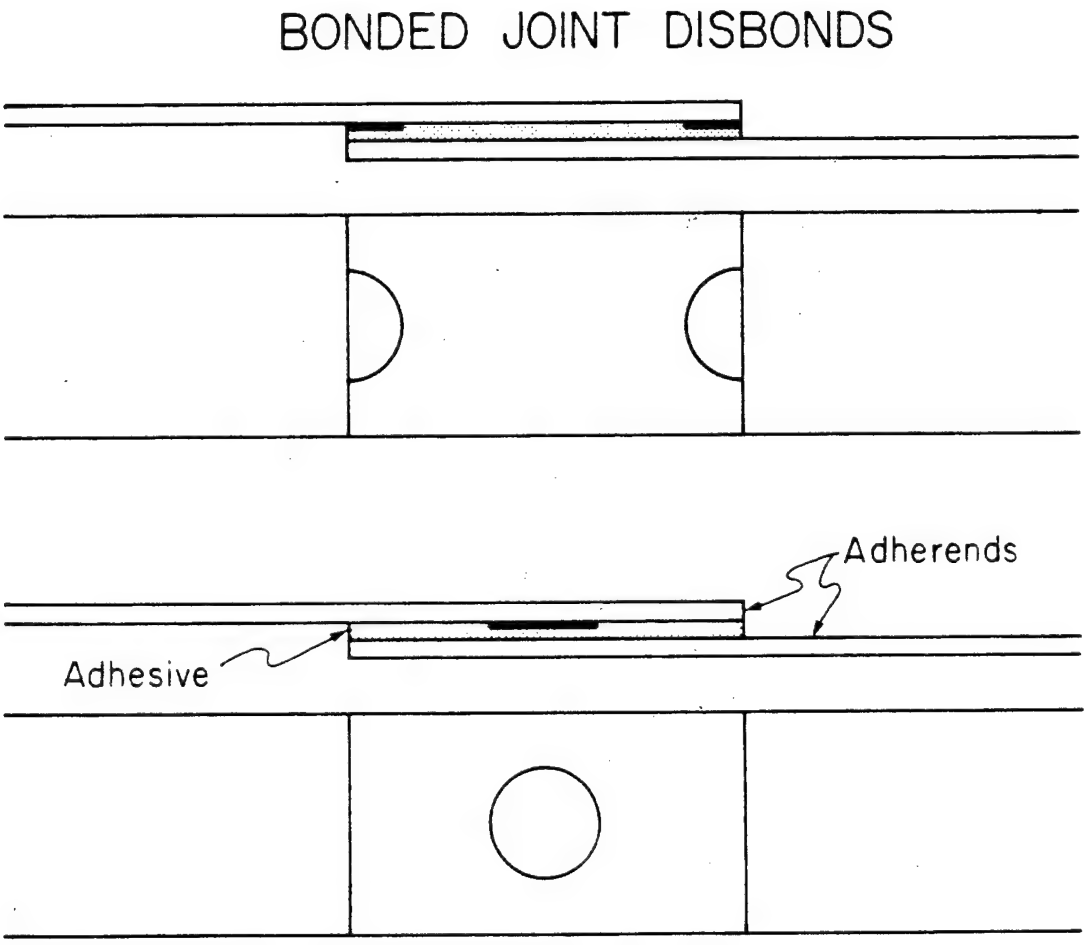

Figure 9 Bonded Joint Test Specimens

the ultrasonic image response as the disbonds were moved through the thickness of the adhesive bond line. It appears that Tedlar is nearly transparent to ultrasonic NDE, at least at 20 MHz. Following this, all subsequent implants are FEP Teflon film.

Quasi-isotropic mechanical data are presented in Table 7. The stress-strain response was monitored using electrical resistance strain gages and all specimens were tested in a screw-driven test machine. Commercial graphite-epoxy Hercules AS1/3501-6 is used for the entire test program.

Table 7

Quasi-isotropic Mechanical Properties
AS1/3501-6

E_{11} = 49.84 GPa

ν_{12} = 0.32

X_1^T = 560 MPa

REFERENCES

1. Chatterjee, S. N., "Composite Defect Criticality", MSC TPR 1403/1109A, Prepared for NADC, Warminster, PA, March 1983.

2. Chatterjee, S. N., and Piper R. B., "Study of Graphite/ Epoxy Composites for Material Flaw Criticality", NADC 78241-60 November 1980.

3. Chatterjee, S. N., and Pipes R. B., "Composite Defect Significance", NADC 80048-60, August 1981.

4. Chatterjee, S. N., Pindera, M. J., Pipes, R. B., and Dick B, "Composite Defect Significance", NADC 81034-60, November 1982.

APPENDIX - A1

3-D ELASTICITY SOLUTION FOR MULTIPLE ELLIPTIC DISBONDS IN A LAMINATED PLATE.

Statement of the Problem

A cluster of elliptic disbonds in a laminated plate of large size subjected to either equal and opposite surface tractions on both faces of each disbond or self-equilibrating tractions on top and bottom surfaces of the laminate over a finite area is considered. It is assumed that the edges of the plate are far away from the delaminations, so that the plate may be considered infinite in x, y directions (fig. 1). The laminate consists of a finite number of layers all of which are homogeneous and elastic. A layer may be a unidirectionally reinforced fiber composite or an isotropic material. The unidirectionally reinforced materials are assumed to be transversely isotropic in planes perpendicular to the fiber directions which lie in planes parallel to the laminate surfaces, but may be orientated at an arbitrary angle.

Solution of the Equations for a Layer

The equations of three dimensional elasticity for each layer of a given laminate are given by

$$\sigma_{jk,k} = 0 \qquad (1) \qquad\qquad \sigma_{jk} = C_{jk\ell m} u_{\ell,m} \qquad (2)$$

Using Latin suffixes j,ℓ which take values 1, 2, 3 and Greek suffixes α,β which take values 1, 2 substitution of (1) in (2) yields.

$$C_{j\alpha\ell\beta} u_{\ell,\alpha\beta} + (C_{j\alpha\ell 3} + C_{j3\ell\alpha})\ u_{\ell,\alpha 3} + C_{j3\ell 3} u_{\ell,33} = 0 \qquad (3)$$

Note that $C_{jk\ell m} = C_{np}$

where (n=j if j=k) or (n=9-j-k if j≠k)

(p=ℓ if ℓ=m) or (p=9-ℓ-m if ℓ≠m) (4)

Taking Fourier transforms in x_1, x_2 directions

$$\tilde{u}_\ell(\underline{\xi}, x_3) = \frac{1}{2\pi} \int_{-\infty}^{\infty} \int_{-\infty}^{\infty} u_\ell(\underline{x}, x_3)\, e^{i\underline{x}\cdot\underline{\xi}} dx_1 dx_2 \tag{5}$$

where $\underline{x} = (x_1, x_2)$ and $\underline{\xi} = (\xi_1, \xi_2)$ are vectors

Inverse of (5) is given by

$$u_\ell(\underline{x}, x_3) = \frac{1}{2\pi} \int_{-\infty}^{\infty} \int_{-\infty}^{\infty} \tilde{u}_\ell(\underline{\xi}, x_3)\, e^{-i\underline{x}\cdot\underline{\xi}} d\xi_1 d\xi_2 \tag{6}$$

Substitution of (6) in (3) yields

$$C_{j313}\tilde{u}_{\ell,33} - i\xi_\alpha(C_{j\alpha\ell 3} + C_{j3\ell\alpha})\,\tilde{u}_{\ell,3} - \xi_\alpha\xi_\beta C_{j\alpha\ell\beta}\tilde{u}_\ell = 0 \tag{7}$$

General solution of (7) is

$$\tilde{u}_\ell(\underline{\xi}, x_3) = \sum_{q=1}^{6} \{A_{\ell q}(\underline{\xi})\, e^{i\lambda_q(\underline{\xi})x_3}\} B_q(\underline{\xi}) \tag{8}$$

where

$$[C_{j3\ell 3}\lambda_q^2 - (C_{j\alpha\ell 3} + C_{j3\ell\alpha})\,\xi_\alpha\lambda_q + \xi_\alpha\xi_\beta C_{j\alpha\ell\beta}]A_{\ell q}(\underline{\xi}) = 0 \tag{9}$$

$$q = 1, \quad 6$$

λ_q are therefore the roots of

$$\text{Det. } [C_{j3\ell 3}\lambda_q^2 - (C_{j\alpha\ell 3} + C_{j3\ell\alpha})\xi_\alpha\lambda_q + \xi_\alpha\xi_\beta C_{j\alpha\ell\beta}] = 0 \tag{10}$$

λ_q's are either purely imaginary or complex and occur in complex conjugate pairs. Therefore, let

$$\lambda_{q+3} = \bar{\lambda}_q \; ; \quad q = 1, 2, 3 \tag{11}$$

For layers of unidirectionally reinforced composites which are transversely isotropic in the plane perpendicular to the fibers the roots can be expressed in simpler form by utilizing the following transformations (fig. 1).

$$\begin{bmatrix} x_1 \\ x_2 \end{bmatrix} = \begin{bmatrix} \cos\theta & -\sin\theta \\ \sin\theta & \cos\theta \end{bmatrix} \begin{bmatrix} x_1' \\ x_2' \end{bmatrix}$$

$$\begin{bmatrix} \xi_1 \\ \xi_2 \end{bmatrix} = \begin{bmatrix} \cos\theta & -\sin\theta \\ \sin\theta & \cos\theta \end{bmatrix} \begin{bmatrix} \xi_1' \\ \xi_2' \end{bmatrix} \tag{12}$$

Where θ is the angle between the fiber direction and x_1 axis. This yields

$$\underline{x} \cdot \underline{\xi} = \underline{x}' \cdot \underline{\xi}' \tag{13}$$

Introducing displacement variables U_ℓ' in x_1', x_2', x_3 direction. Where x_1' coincides with the direction of fibers so that

$$\begin{bmatrix} u_1 \\ u_2 \\ u_3 \end{bmatrix} = \begin{bmatrix} \cos\theta & -\sin\theta & 0 \\ \sin\theta & \cos\theta & 0 \\ 0 & 0 & 1 \end{bmatrix} \begin{bmatrix} u_1' \\ u_2' \\ u_3' \end{bmatrix} \tag{14}$$

one obtains for transform variables $\tilde{u}_\ell'$

$$\tilde{u}_\ell'(\underline{\xi}, x_3) = \tilde{u}_\ell'(\underline{\xi}, x_3) = \frac{1}{2\pi} \int_{-\infty}^{\infty} \int_{-\infty}^{\infty} u_\ell'(\underline{x}, x_3) e^{i\underline{x}' \cdot \underline{\xi}'} dx_1' dx_2' \tag{15}$$

Where,

$$\tilde{u}_{\ell}(\underline{\xi},x_3) = \sum_{q=1}^{6} \{A_{\ell q}(\underline{\xi}) e^{i\lambda_q(\underline{\xi})x_3}\} B_q(\underline{\xi}) \tag{16}$$

The roots λ_q^2 are given by

$$\lambda_q^2 = -[\xi_1^2/\kappa_q^2 + \xi_2^2] \tag{17}$$

Where

$$\kappa_q^2 = \frac{1}{2}\left[\kappa' \pm \sqrt{\kappa'^2 - 4C_{22}/C_{11}}\right], \quad q = 1, 2$$

$$\kappa' = (C_{11}C_{22} - C_{12}^2 - 2C_{12}C_{55})/C_{11}C_{55} \tag{18}$$

$$\kappa_3^2 = C_{44}/C_{55}$$

C_{ij} being the engineering stiffnesses in contracted notations, direction 1 conciding with the fiber direction and C_{55} and C_{44} denoting the axial and transverse sheer moduli respectively. The six roots λ_q are therefore given by

$$\lambda_q = -i\lambda'_q \quad , q = 1, 2, 3$$

$$\text{and} \quad \lambda_{q+3} = i\lambda'_q = \bar{\lambda}_q \tag{19}$$

$$\text{where,} \quad \lambda'_q = \sqrt{\xi_1'^2/\kappa_q^2 + \xi_1'^2}$$

For commonly used fiber composites the roots are all distinct and $A'_{\ell q}$ in (16) can be expressed as

$$A'_{1q} = \xi'_1, \quad A'_{2q} = A_q^* \xi'_2, \quad A'_{3q} = -iA_q^* \lambda'_q, \quad q = 1, 2$$

$$\text{where,} \quad A_q^* = (C_{12} + C_{55})/(C_{55} - C_{22}/\kappa_q^2) \tag{20}$$

$$A'_{13} = 0, \quad A_{23} = -\lambda'_3, \quad A'_{33} = -i\xi'_2$$

and $$A'_{\ell(q+3)} = \bar{A}'_{\ell q} \tag{21}$$

Hence, it follows that equation (16) can be written as

$$\tilde{u}'_{\ell}(\underline{\xi}', x_3) = \frac{1}{2} \sum_{q=1}^{3} \left[A'_{\ell q} B'_q \ell^{\lambda' q x_3} + \bar{A}'_{\ell q} B'_{q+3} \ell^{-\lambda' q x_3} \right] \tag{22}$$

For a layer deforming symmetrically (c=1) and antisymmetrically (c=2) about the midplane $x_3=0$ the following solutions are obtained by taking $B'_{q+3} = B'_q$ for c=1 and $B'_{q+3} = -B'_q$ for c=2.

$$\begin{aligned} \tilde{u}'^{c}_{\ell} &= \sum_{q=1}^{3} B'^{c}_q A'_{\ell q} F^{c}_{1q}(x_3) \; ; \; \ell = 1, 2 \\ i\tilde{u}'^{c}_{3} &= \sum_{q=1}^{3} B'^{c}_q A''_{3q} F^{c}_{2q}(x_3) \end{aligned} \tag{23}$$

Where $A''_{3q} = iA'_{3q}$, A'_{3q} being given by (20) and the functions F^{c}_{mq} , c = 1, 2 are as follows

	Case 1 (C=1)	Case 2 (C=2)
F^{c}_{1q} =	$\cosh \lambda'_Q x_3$	$\sinh \lambda'_Q x_3$
F^{c}_{2q} =	$\sinh \lambda'_Q x_3$	$\cosh \lambda'_q x_3$

(24)

Relationship of Boundary Tractions and Displacements

The transformed tractions at the boundary $z = + \frac{h}{2}$ of the layer are related to the transformed displacements at $z = + \frac{h}{2}$ by the following relations.

$$\overset{c}{\underset{\sim}{T}}\left(+\frac{h}{2}\right)=\begin{bmatrix} \overset{c}{\underset{\sim}{\sigma}}_{31}\left(+\frac{h}{2}\right) \\ \overset{c}{\underset{\sim}{\sigma}}_{32}\left(+\frac{h}{2}\right) \\ i\overset{c}{\underset{\sim}{\sigma}}_{33}\left(+\frac{h}{2}\right) \end{bmatrix} = \begin{bmatrix} \overset{c}{k}_{11} & \overset{c}{k}_{12} & \overset{c}{k}_{13} \\ \text{sym.} & \overset{c}{k}_{22} & \overset{c}{k}_{23} \\ & & \overset{c}{k}_{33} \end{bmatrix} \begin{bmatrix} \overset{c}{\underset{\sim}{u}}_1\left(+\frac{h}{2}\right) \\ \overset{c}{\underset{\sim}{u}}_2\left(+\frac{h}{2}\right) \\ i\overset{c}{\underset{\sim}{u}}_3\left(+\frac{h}{2}\right) \end{bmatrix} = [\overset{c}{K}] \overset{c}{\underset{\sim}{U}}\left(+\frac{h}{2}\right) \tag{25}$$

where,

$$\Delta \overset{c}{k}_{11} = C_{55}\left[\lambda_2\lambda_2\lambda_3 (A_2^* - A_1^*) f_1 f_2 + \xi_2^2 (A_1^*\lambda_2 f_2 - A_2^*\lambda_1 f_1) f_3\right]$$

$$\Delta \overset{c}{k}_{12} = C_{55}\, \xi_1 \xi_2 (\lambda_2 f_2 - \lambda_1 f_1)\, f_3$$

$$\Delta \overset{c}{k}_{13} = C_{55}\, \xi_1\left[-\lambda_1\lambda_3(1 - A_1^*) f_1 + \lambda_2\lambda_3(1 - A_2^*) f_2 - \xi_2^2 (A_1^* - A_2^*) f_3\right]$$

$$\Delta \overset{c}{k}_{22} = C_{55}\, \xi_1^2 (A_2^*\lambda_2 f_2 - A_1^*\lambda_1 f_1)\, f_3 \tag{26}$$

$$\Delta \overset{c}{k}_{23} = C_{44}\, \xi_2\left[2\lambda_3(\lambda_1 A_1^* f_1 - \lambda_2 A_2^* f_2) - (\lambda_3^2 + \xi_2^2)\, (A_1^* - A_2^*) f_3\right]$$

$$\Delta \overset{c}{k}_{33} = C_{55}\, \xi_1^2\, \lambda_3\, (A_2^* - A_1^*)$$

and $\overset{c}{\Delta} = \lambda_3\, (\lambda_2 A_2^* f_2 - \lambda_1 A_1^* f_1) + \xi_2^2 (A_1^* - A_2^*)\, f_3$

and f_j, $j = 1, 2, 3$ are given by

	Case 1 (c=1)	Case 2 (c=2)
$f_j =$	$\tanh \lambda_q \frac{h}{2}$	$\coth \lambda_q \frac{h}{2}$

The quantities ξ_1', ξ_2' and λ_q' etc. in equation (27) can be expressed as

$$\xi_1' = \xi_1 \cos\theta + \xi_2 \sin\theta, \qquad \xi_2' = -\xi_1 \sin\theta + \xi_2 \cos\theta$$

$$\begin{aligned}
\xi_1'^2 &= \xi_1^2 \cos^2\theta + \xi_2^2 \sin^2\theta + 2\xi_1\xi_2 \sin\theta \cos\theta', \\
\xi_2'^2 &= \xi_2'^2 \sin^2\theta + \xi_2^2 \cos^2\theta - 2\,\xi_1'\xi_2 \sin\theta \cos\theta \\
\xi_1'\,\xi_2' &= (-\xi_1^2 + \xi_2^2) \sin\theta \cos\theta + \xi_1\xi_2 \cos 2\theta \text{ and}
\end{aligned} \tag{27}$$

$$\lambda_q' = \sqrt{\xi_1^2\left(\frac{\cos^2\theta}{\kappa_q^2} + \sin^2\theta\right) + \xi_2^2\left(\frac{\sin^2\theta}{\kappa_q^2} + \cos^2\theta\right) + 2\,\xi_1\xi_2\left(\frac{1}{\kappa_q^2} - 1\right)\sin\theta\cos\theta}$$

Transformed tractions in x_1, x_2, x_3 coordinate systems are related to the corresponding displacements by

$$[\tilde{\underline{T}}\ (+\tfrac{h}{2})] = [\overset{c}{K}]\ [\tilde{\underline{U}}\ (+\tfrac{h}{2})] \tag{28}$$

where

$$\overset{c}{k}_{11} = \frac{\left(\overset{c'}{k}_{11} + \overset{c'}{k}_{22}\right)}{2} + \frac{\overset{c'}{k}_{11} - \overset{c'}{k}_{22}}{2} \cos 2\theta - \overset{c'}{k}_{12} \sin 2\theta$$

$$\overset{c}{k}_{12} = \frac{\overset{c'}{k}_{11} - \overset{c'}{k}_{22}}{2} \sin 2\theta + \overset{c'}{k}_{12} \cos 2\theta$$

$$\overset{c}{k}_{13} = \overset{c'}{k}_{13} \cos\theta - \overset{c'}{k}_{23} \sin\theta \tag{29}$$

$$\overset{c}{k}_{22} = \frac{\overset{c'}{k}_{11} + \overset{c'}{k}_{22}}{2} - \frac{\overset{c'}{k}_{11} - \overset{c'}{k}_{22}}{2} \cos 2\theta + K_{12}' \sin 2\theta$$

$$\overset{c}{k}_{23} = \overset{c'}{k}_{13} \sin\theta + \overset{c}{k}_{23} \cos\theta$$

$$\overset{c}{k}_{33} = \overset{c'}{k}_{33}$$

Now a general case of loading on the layer can be written as a sum of symmetric and antisymmetric loadings. Let the transformed tractions $[\tilde{t}_1, \tilde{t}_2, i\tilde{t}_3]^{tr}$ at $z = +\frac{h}{2}$ be denoted as $\underset{\sim}{T}_1$, where t_1, t_2, and t_3 are in +ve x_1, x_2, x_3 directions and $[\tilde{u}_1, \tilde{u}_2, i\tilde{u}_3]^{tr}$ at $z = +\frac{h}{2}$ be expressed as $\underset{\sim}{\tilde{U}}_1$. Let the corresponding quantities at $z = -\frac{h}{2}$ be written as $\underset{\sim}{\tilde{T}}_2$ and $\underset{\sim}{\tilde{U}}_2$ respectively. Then one can write

$$\begin{aligned} \underset{\sim}{T}_1 &= \overset{11}{[K]}\, \underset{\sim}{U}_1 + \overset{12}{[K]}\, \underset{\sim}{U}_2 \\ T_2 &= \overset{21}{[K]}\, \underset{\sim}{U}_1 + \overset{22}{[K]}\, \underset{\sim}{U}_2 \end{aligned} \tag{30}$$

where

$$\overset{11}{[K]} = \begin{bmatrix} (\overset{1}{k}_{11} + \overset{2}{k}_{11})(\overset{1}{k}_{12} + \overset{2}{k}_{12})(\overset{1}{k}_{13} + \overset{2}{k}_{13}) \\ (\overset{1}{k}_{22} + \overset{2}{k}_{22})(\overset{1}{k}_{23} + \overset{2}{k}_{23}) \\ \text{sym.} \quad (\overset{1}{k}_{33} + \overset{2}{k}_{33}) \end{bmatrix}$$

$$\overset{12}{[K]} = \begin{bmatrix} (\overset{1}{k}_{11} - \overset{2}{k}_{11})(\overset{1}{k}_{12} - \overset{2}{k}_{12})(-\overset{1}{k}_{13} + \overset{2}{k}_{13}) \\ (\overset{1}{k}_{12} - \overset{2}{k}_{12})(\overset{1}{k}_{22} - \overset{2}{k}_{22})(-\overset{1}{k}_{23} + \overset{2}{k}_{23}) \\ (\overset{1}{k}_{13} - \overset{2}{k}_{13})(\overset{1}{k}_{23} - \overset{2}{k}_{23})(-\overset{1}{k}_{33} + \overset{2}{k}_{33}) \end{bmatrix} \tag{31}$$

$$\overset{21}{[K]} = \overset{12}{[K]}^{tr}$$

and elements of $\overset{22}{[K]}$ are obtained from these of $\overset{11}{[K]}$ by changing the signs of $\overset{11}{k}_{13}$, $\overset{11}{k}_{23}$, $\overset{11}{k}_{31}$, and $\overset{11}{k}_{32}$. Expressions for $\overset{1}{k}_{ij}$ and $\overset{2}{k}_{ij}$ are given by (29), (26) and (27).

Satisfaction of Interface Conditions

At an interface ℓ between $(\ell-1)^{th}$ and ℓ^{th} layer $(1<\ell<n)$ without any disbonds the displacement vectors of two adjacent layers above and below the interface must be identical and the corresponding traction vectors must add up to zero. Note that 1 and n indicate the top and bottom surfaces of the laminate where tractions are either zero or have a prescribed value. Let $\underline{V}_\ell$ denote the displacement vector at all such interfaces.

At interfaces ℓ_j (j = 1, 2..m), containing disbonds

$$\text{let} \qquad \underline{U}_2^{\sim \ell_j - 1} = \underline{\tilde{V}}_{\ell_j} + [K^0_{\ell_j}]\ [K^{11*}_{\ell_j}]\ \underline{\tilde{V}}^*_j \tag{32}$$

$$\text{and} \qquad \underline{U}_1^{\sim \ell_j} = \underline{\tilde{V}}_{\ell_j} - [K^0_{\ell_j}]\ [K^{22*}_{\ell_j - 1}]\ \underline{\tilde{V}}^*_j$$

The superscript on $\underline{\tilde{U}}$ in the left hand sides of (32) indicates the layer and the subscripts 1 and 2 stand for top and bottom surfaces of that layer. $\underline{\tilde{V}}^*_j$ in the right hand side of the equation is the transform of the displacement discontinuity vector at interface $\ell_j (= \tilde{U}_2^{\ell_j - 1} - \tilde{U}_1^{\ell_j})$. $K^{\alpha\beta *}_{\ell_j}$ is the asymptotic form of the stiffness matrix $[K^{\alpha\beta}_{\ell_j}]$ of layer ℓ_j, i.e. the limiting form as the layer thickness h approaches infinity. Note that if one writes $[\xi_1, \xi_2] = [\xi\cos\phi \quad \xi\sin\phi]$

$$\text{then,} \qquad [K^{\alpha\beta *}] = \xi^{\alpha\beta}[F(\phi)] \tag{33}$$

where the elements f_{11}, f_{22}, f_{12}, f_{22}, f_{33} of [F] behave in the following manner

$$f_{11}(\pi+\phi) = f_{11}(\phi) \tag{34a}$$

and the elements f_{13} and f_{23} satisfy the relationship.

$$f_{13}(\pi+\phi) = -f_{13}(\phi) \tag{34b}$$

The matrix $[K^*_{\ell_j}]$ in (32) is given by

$$[K^{0}_{\ell_j}] = [K^{-1\ 11*}_{\ell_j}] + [K^{22*}_{\ell_j-1}] \tag{35}$$

Since the tractions on the top and bottom disbond surfaces are either zero or equal and opposite the traction vectors at such an interface ℓ_j acting on the adjacent layers add up to zero as in the case of interfaces without any disbonds. In view of (32) these conditions can therefore by written as

$$\underset{3n\times 3n}{[K^G]} \begin{bmatrix} \underset{\sim}{V}_1 \\ \\ \underset{\sim}{V}_{\ell_j} \\ \\ \underset{\sim}{V}_n \end{bmatrix} = \underset{3n\times 3m}{[B]} \begin{bmatrix} \underset{\sim}{V}^*_1 \\ \cdot \\ \cdot \\ \cdot \\ \underset{\sim}{V}^*_j \\ \cdot \\ \cdot \\ \cdot \\ \underset{\sim}{V}^*_m \end{bmatrix} + \begin{bmatrix} \underset{\sim}{T}_1 \\ 0 \\ 0 \\ \cdot \\ \cdot \\ \cdot \\ \cdot \\ \underset{\sim}{T}_n \end{bmatrix} \tag{36}$$

The matrix K^G is the global stiffness matrix in the transformed domain and is of the following form

$$[K^G] = \begin{bmatrix} K_1^{11} & K_2^{12} & 0 & 0 & 0 & \cdot \\ K_1^{22} + K_2^{11} & K_2^{12} & 0 & 0 & & \cdot \\ & K_2^{22} + K_3^{11} & K_3^{12} & & & \cdot \\ & & & & & \cdot \\ \text{sym.} & & & & & K_n^{22} \end{bmatrix} \tag{37}$$

The matrix B is of size (3n x 3m) and the elements of columns $3\ell_j-2$, $3\ell_j-1$, and $3\ell_j$ are given by,

$$
\begin{array}{lc}
 & \vdots \\
 & 0 \\
\text{Rows } 3\ell_j-3 \to 3\ell_j-1 & -[K^{12}_{\ell_j-1}]\ [K^{0}_{\ell_j}]\ [K^{11}_{\ell_j}] \\
\text{Rows } 3\ell_j-2 \to 3\ell_j & [K^{11}_{\ell_j}]\ [K^{0}_{\ell_j}]\ [K^{22*}_{\ell_j-1}] - [K^{22}_{\ell_j-1}]\ [K^{0}_{\ell_j}]\ [K^{11*}_{\ell_j}] \\
\text{Rows } 3\ell_j+1 \to 3\ell_j+3 & [K^{21}_{\ell_j}]\ [K^{0}_{\ell_j}]\ [K^{22*}_{\ell_j-1}] \\
 & 0 \\
 & \vdots
\end{array}
\qquad (38)
$$

$\tilde{T}_1$ and $\tilde{T}_n$ are the transforms of applied traction vectors on top and bottom surfaces of the laminate. It should be noted that all elements of B in (38) approach zero expotentially as $\sqrt{\xi_1^2 + \xi_2^2}$ approach infinity.

Equation (36) can be formally solved to express $\tilde{\underline{V}}_\ell$ as

$$\tilde{\underline{V}}_\ell = \sum_{p=1}^{m} [D_{\ell p}]\ \tilde{\underline{V}}^*_p + [E_{\ell 1}]\ \tilde{\underline{T}}_1 + [E_{\ell 2}]\ \tilde{\underline{T}}_n \qquad (39)$$

The transform of the traction vector on the top face of layer ℓ_j (j=1, 2. . m) (corresponding to bottom surface of disbonded interface ℓ_j) can, therefore, be written (with the help of (30), (32), and (39)) as

$$\tilde{\underline{T}}^{\ell_j}_1 = \tilde{\underline{T}}^*_j = [K^{11}_{\ell_j}]\ \tilde{\underline{U}}^{\ell_j}_1 + [K^{12}_{\ell_j}]\ \tilde{\underline{U}}^{\ell_j}_2 \qquad (40)$$

or, $$\tilde{\underline{T}}^*_j = [C^{*j}]\ \tilde{\underline{V}}^*_j + \sum_{p=1}^{m} [C^{jp}]\ \tilde{\underline{V}}^*_p + \tilde{\underline{T}}^0_j \qquad (41)$$

where $$[C_j^*] = -[K_{\ell_j}^{11*}][K_{\ell_j}^{0}][K_{\ell_{j-1}}^{22*}] \tag{42}$$

$$[C_{jp}] = [K_{\ell_j}^{11}][D_{\ell_{jp}}] + [K_{\ell_j}^{12}][D_{(\ell_{j+1})p}] \tag{43}$$

$$+[K_{\ell_j}^{11*} - K_{\ell_j}^{11}]\,[K_{\ell_j}^{0}]\,[K_{\ell_{j-1}}^{22*}]\,\delta_{jp}$$

$$+[K_{\ell_j}^{12}]\,[K_{\ell_{j+1}}^{0}]\,[K_{\ell_{j+1}}^{11*}]\,\delta_{(j+1)p}\,\delta_{(\ell j+1)\ell_{j+1}}$$

δ_{jp} being the Kronecker delta. The term $\tilde{\underline{T}}_j^0$ is given by

$$\tilde{\underline{T}}_j^0 = [F_{j1}]\,\tilde{\underline{T}}_1 + [F_{j2}]\,\tilde{\underline{T}}_2 \tag{44}$$

$$[F_{jp'}] = [K_{\ell_j}^{11}]\,[E_{\ell_{jp'}}] + [K_{\ell_j}^{12}][E_{(\ell_{j+1})p'}];\ p' = 1,2$$

The elements of $[C^{*j}]$ behave like (33) whereas these of $[C^{jp}]$ approach zero expotentially as $\xi \to \infty$.

$\tilde{\underline{V}}_j^*$, the transform of the displacement discontinuity vector a interface ℓ_j containing Q_j number of elliptic disbonds can be expressed as

$$\tilde{\underline{V}}_j^* = \frac{1}{2\pi} \sum_{q=1}^{Qj} \int_{A_{jq}} V_j^{q*}(\underline{x})\, e^{i\underline{x}\cdot\underline{\xi}}\, dA \tag{45}$$

The inverse transform of equation (41) is therefore,

$$\underline{T}_j^*(\underline{x}') = \frac{1}{2\pi} \int_{-\infty}^{\infty} \int_{-\infty}^{\infty} \tilde{\underline{T}}_j^*\, e^{-i\underline{x}'\cdot\underline{\xi}}\, d\xi_1 d\xi_2$$

$$= \frac{1}{4\pi^2} \sum_{q=1}^{Qj} \int_{-\infty}^{\infty} \int_{-\infty}^{\infty} [C^{*j}]\, \underline{V}_j^{q*}(\underline{x})\, e^{i(\underline{x}-\underline{x}')\cdot\underline{\xi}}\, d\xi_1 d\xi_2 dA \tag{46}$$

$$+ \frac{1}{4\pi^2} \sum_{p=1}^{m} \sum_{q=1}^{Qp} \int_{-\infty}^{\infty} \int_{-\infty}^{\infty} [C^{jp}] \, V_p^{q*} \, e^{i(\underline{x} - \underline{x}').\underline{\xi}} \, d\xi_1 \, d\xi_2 \, dA$$

$$+ \frac{1}{2\pi} \int_{-\infty}^{\infty} \int_{-\infty}^{\infty} \underset{\sim}{T}_j^{o} \, e^{-i\underline{x}'.\underline{\xi}} \, d\xi_1 d\xi_2$$

$$j = 1, 2 \ldots m.$$

Since, the tractions on Q_j disbonds at ℓ_j^{th} interface are either zero or prescribed, equation (46) is a set of integral equations for evaluation of the unknown functions V_j^{q*}; $q = 1, 2, \ldots Q_j$, $j = 1, 2, \ldots m$. For obtaining numerical solution of (46) the elliptic disbonds are mapped on to circular regions and equation (46) is discretized.

Appendix-A2

Representative C-scans of Multiple Delamination Specimens

Gated at C, MC, MT, T (see fig. 4)

for Different Load Cycles

See Figure 4 and Table 2

for Gating Procedure and Specimen

Details

Specimen 1.2-A3, C, MC, MT, T

1.2-A3 C

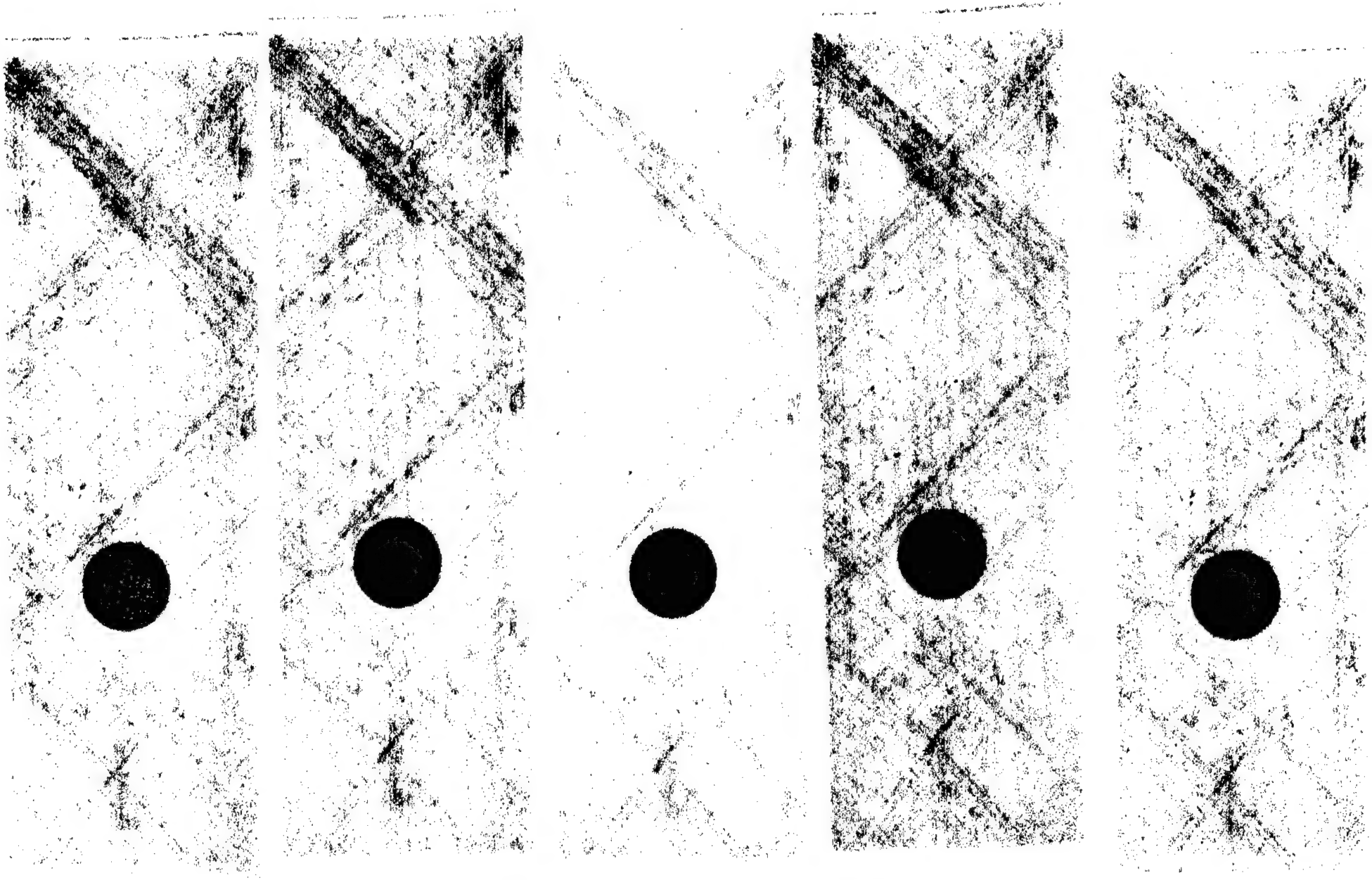

0 3000 10000 15000 18000

1.2-A3 C

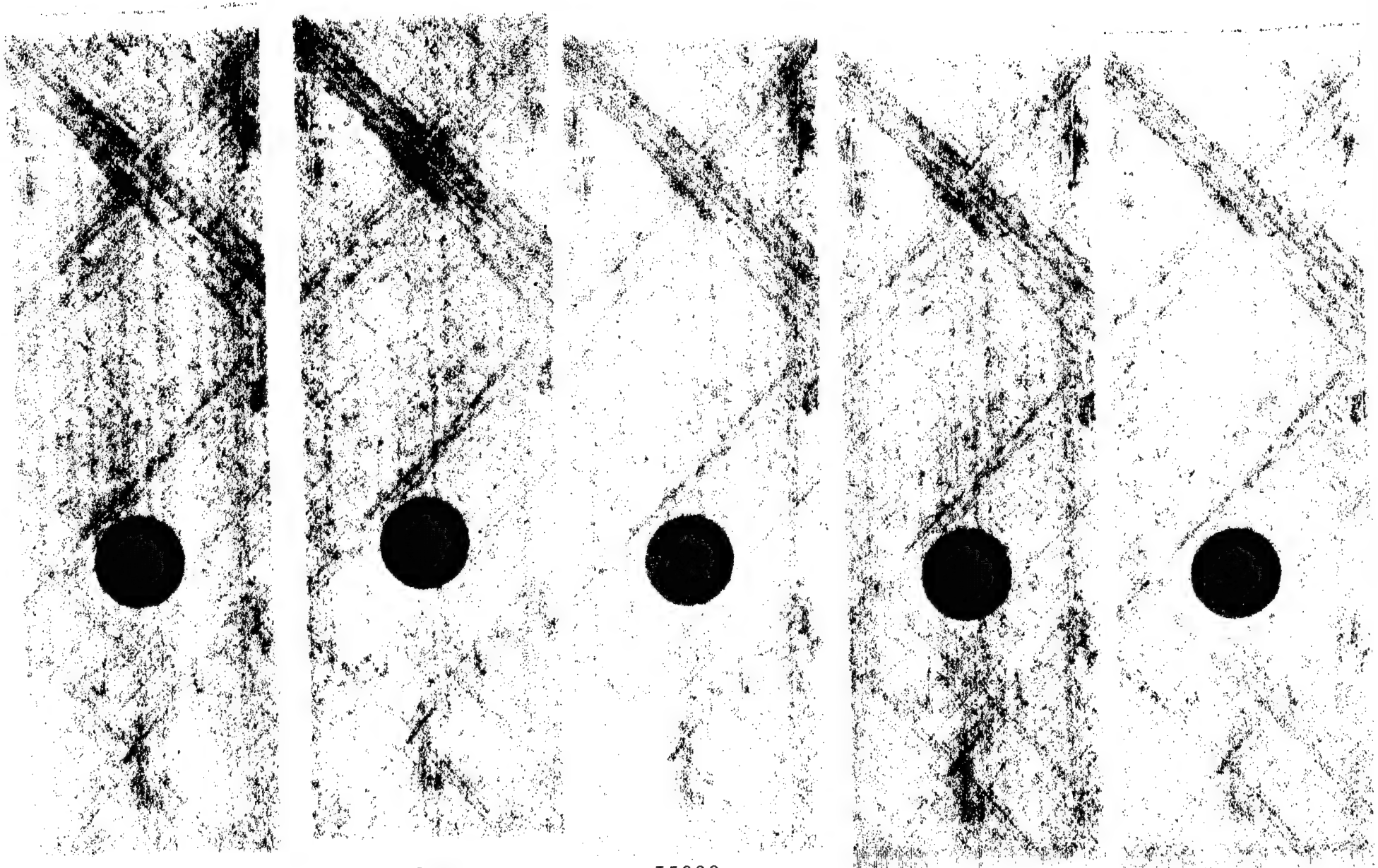

21000 26000 35000 45000 55000

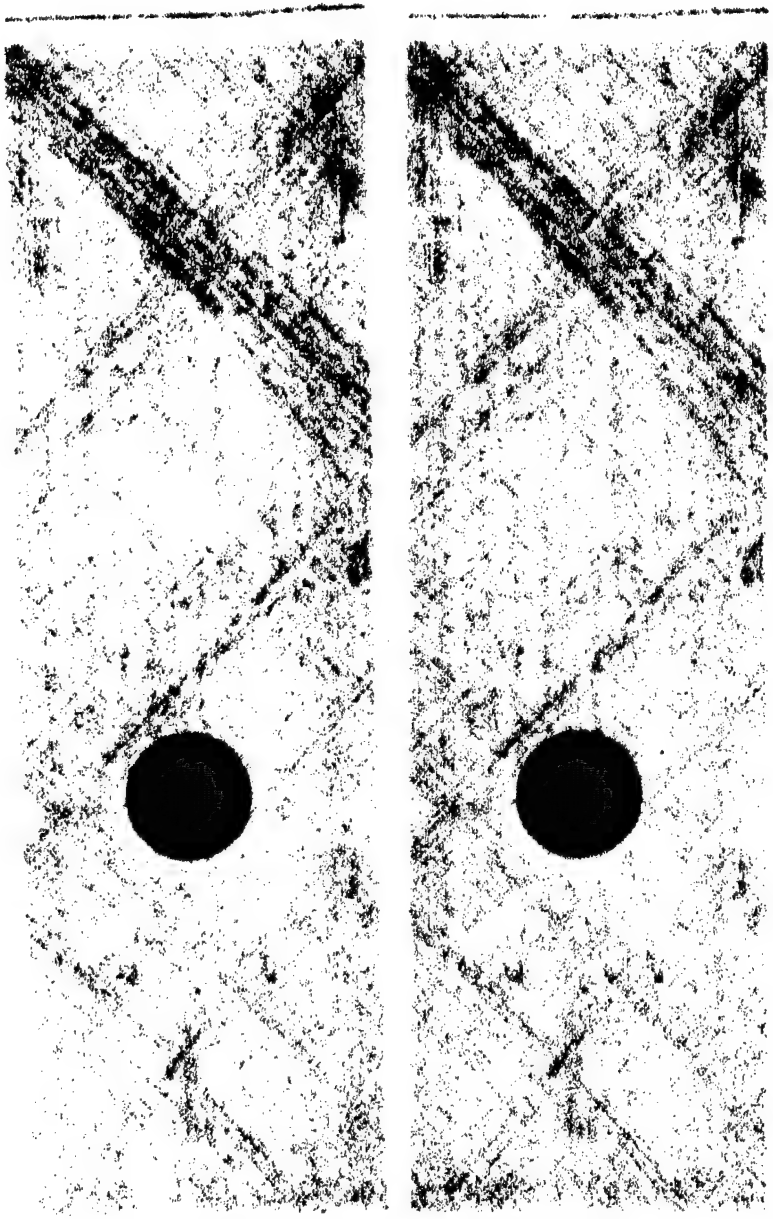

65000 85000

1.2-A3 MC

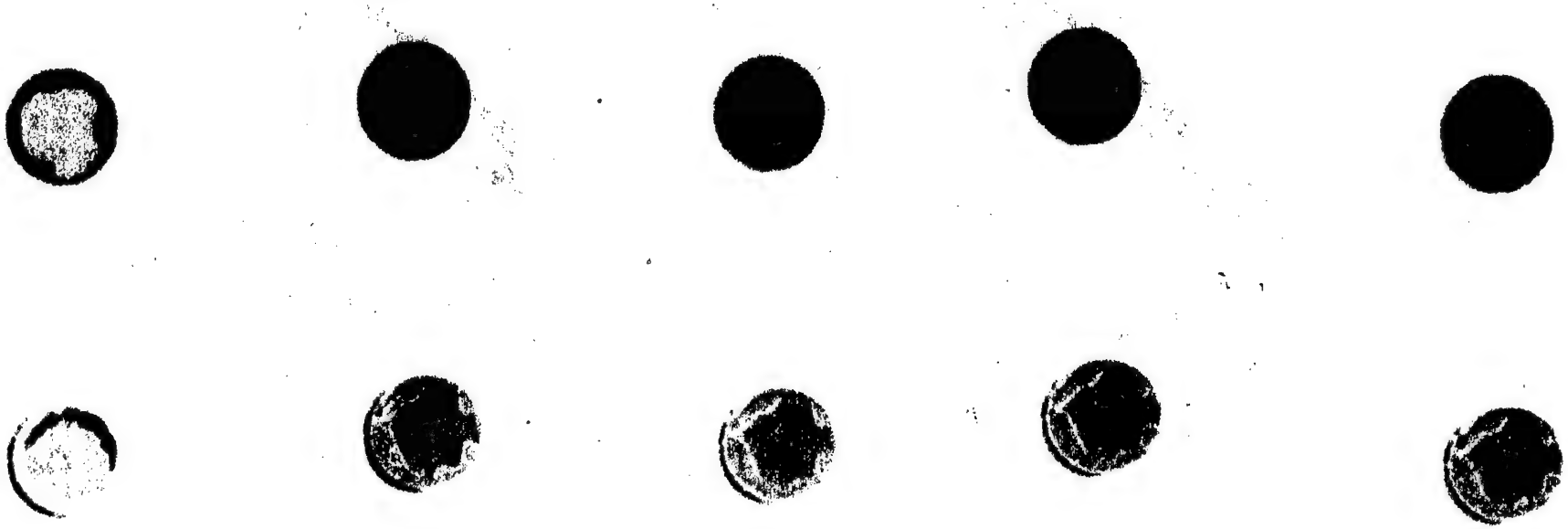

0 3000 10000 15000 18000

1.2-A3 MC

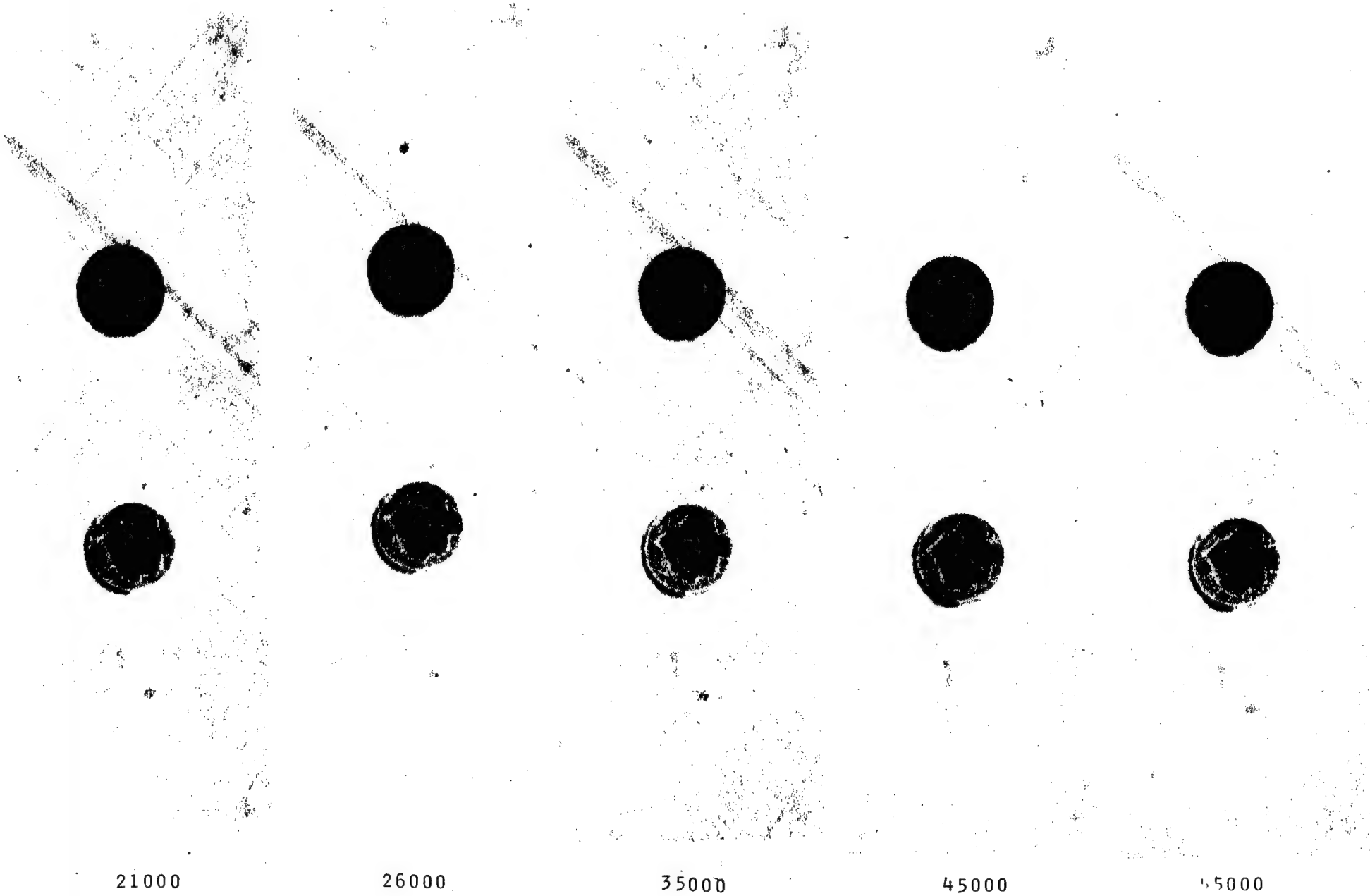

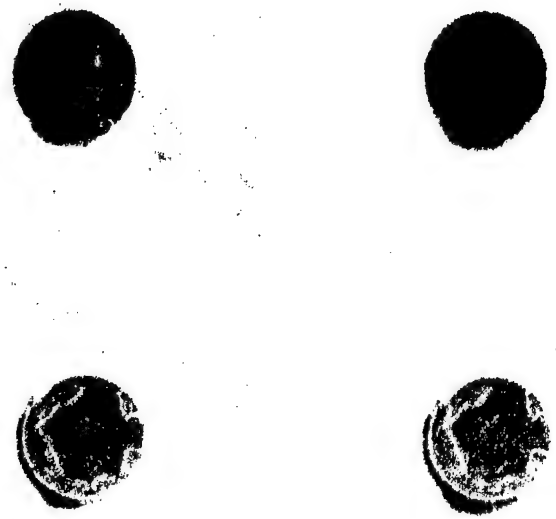

65000 85000

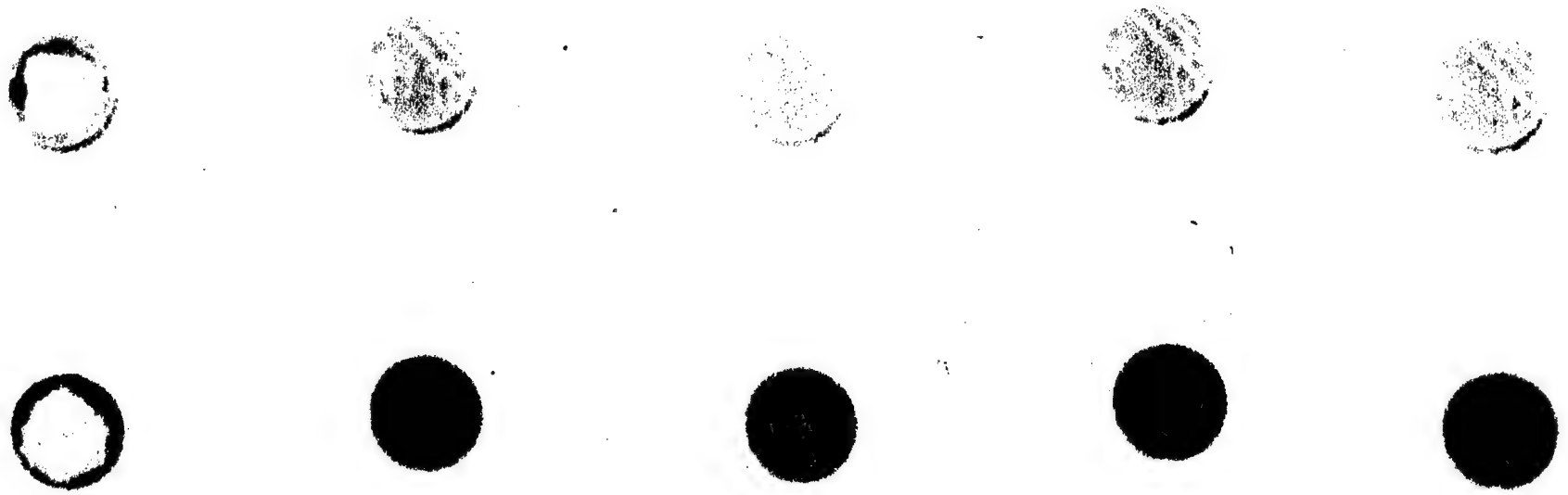

0 3000 10000 15000 18000

1.2-A3 MT

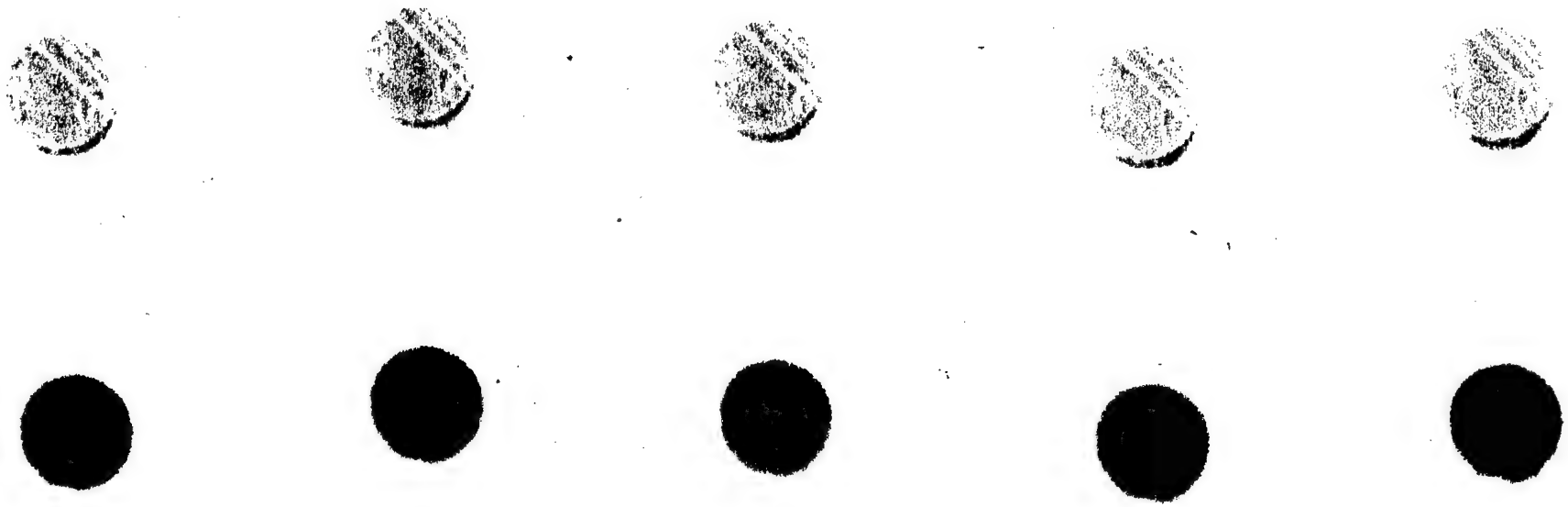

21000 26000 35000 45000 55000

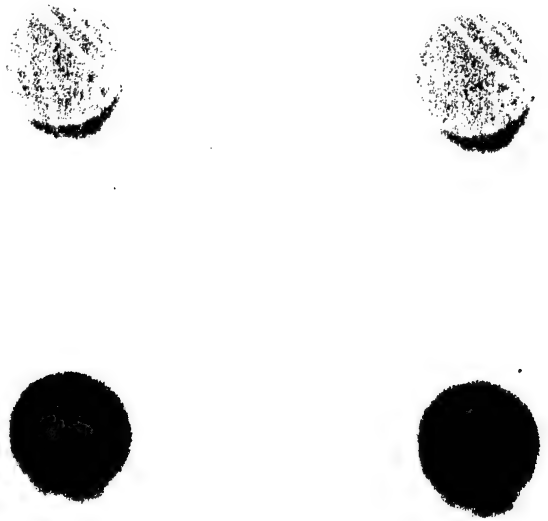

65000 85000

1.2-A3 T

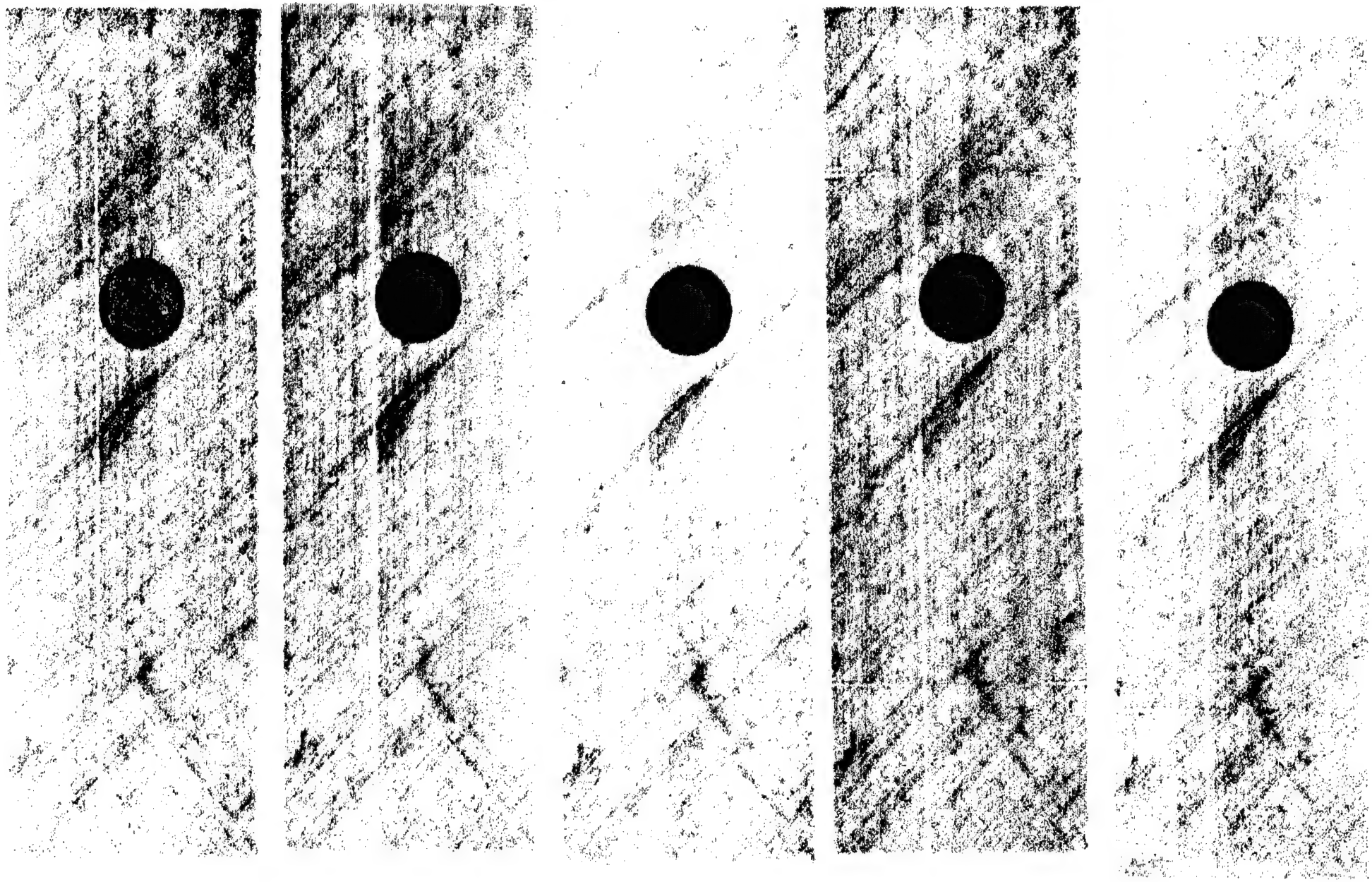

0 3000 10000 15000

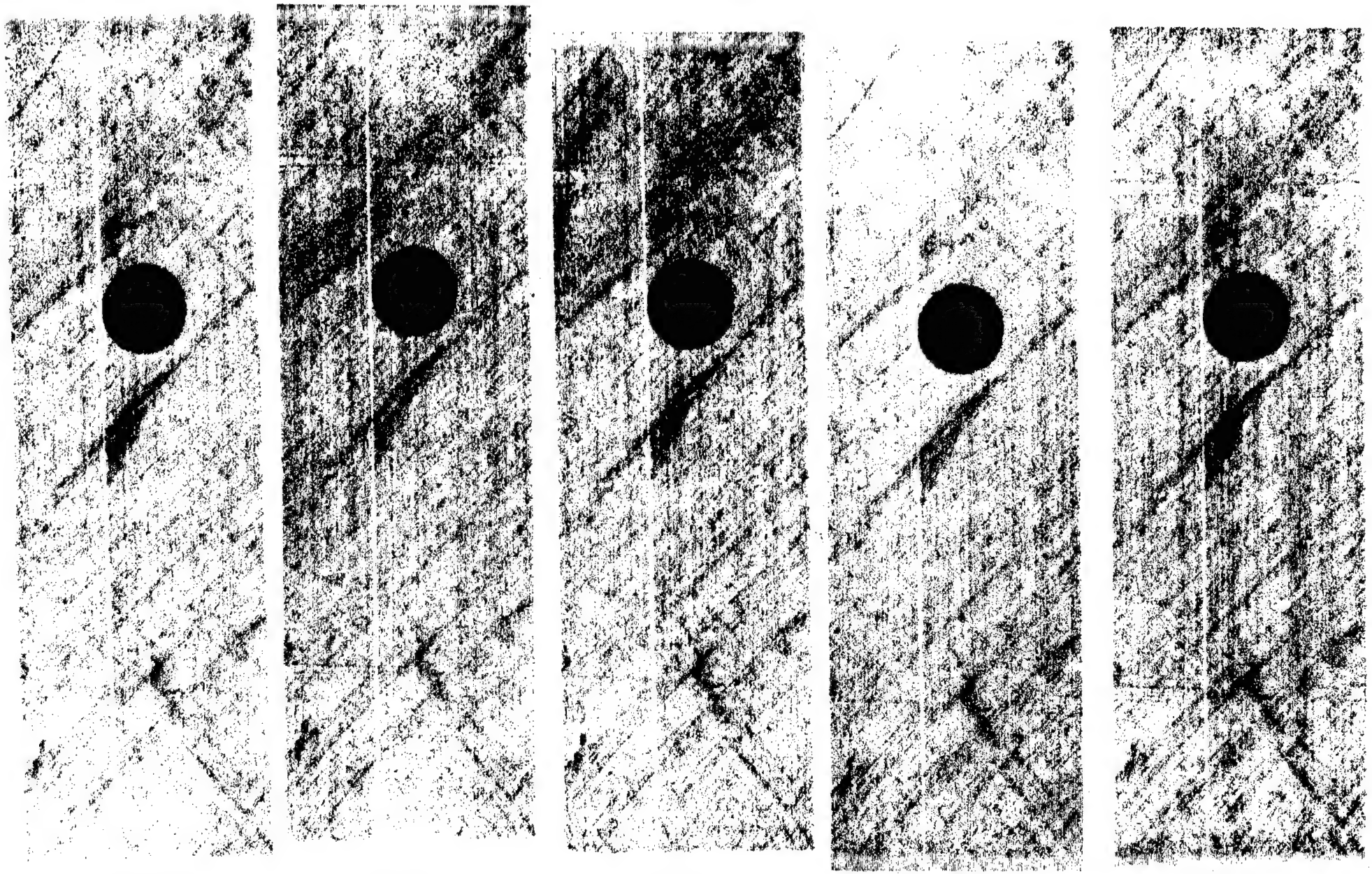

21000 26000 35000 45000 55000

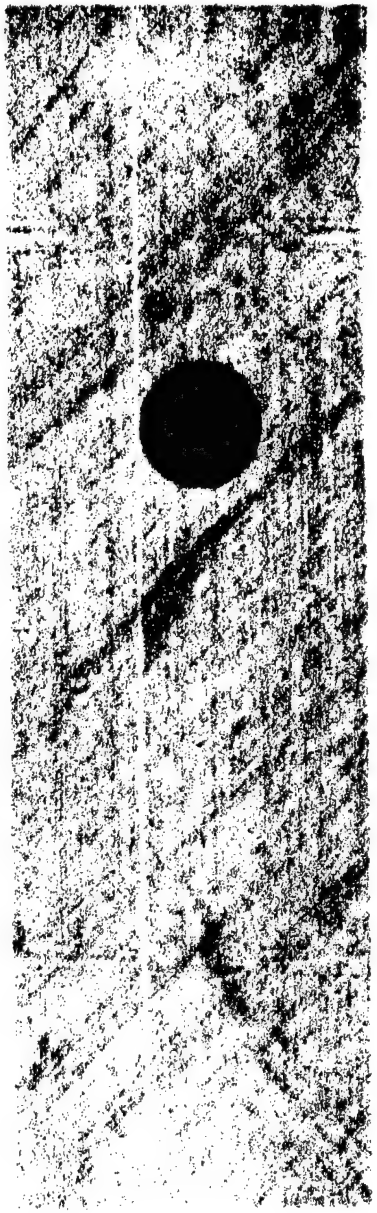

65000

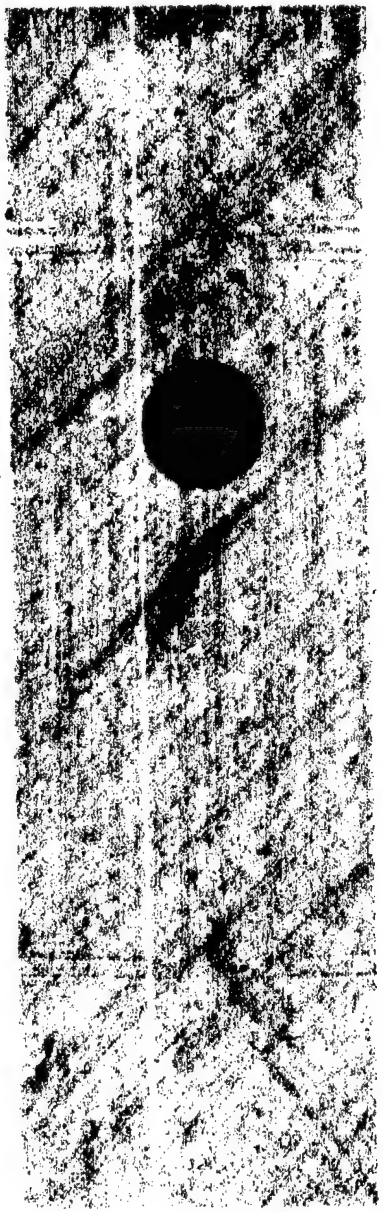

85000

Specimen 1.3-Al C, MC, MT, T

1.3-A1 C

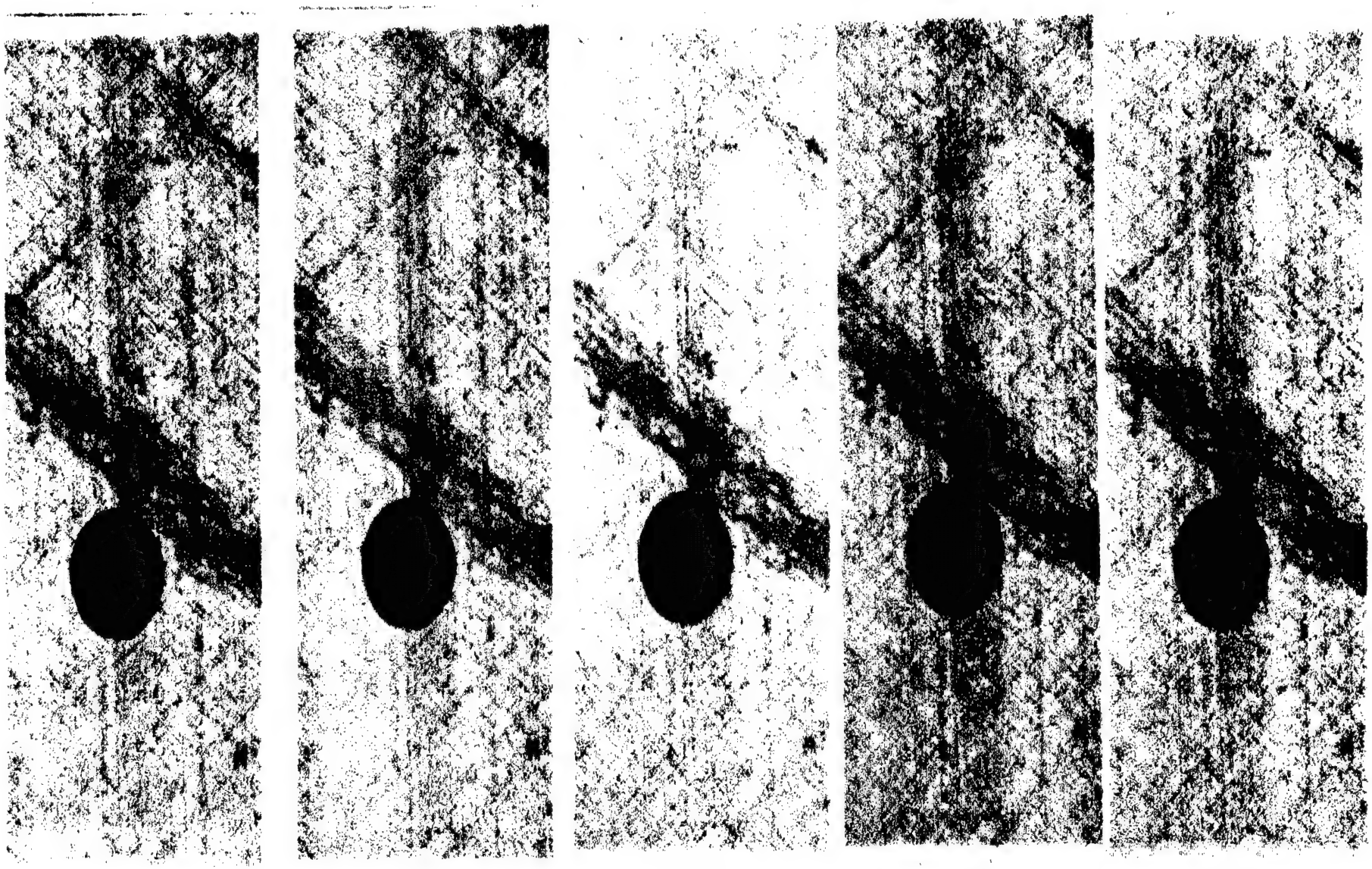

0 3000 10800 13000 18000

1.3-A1 C

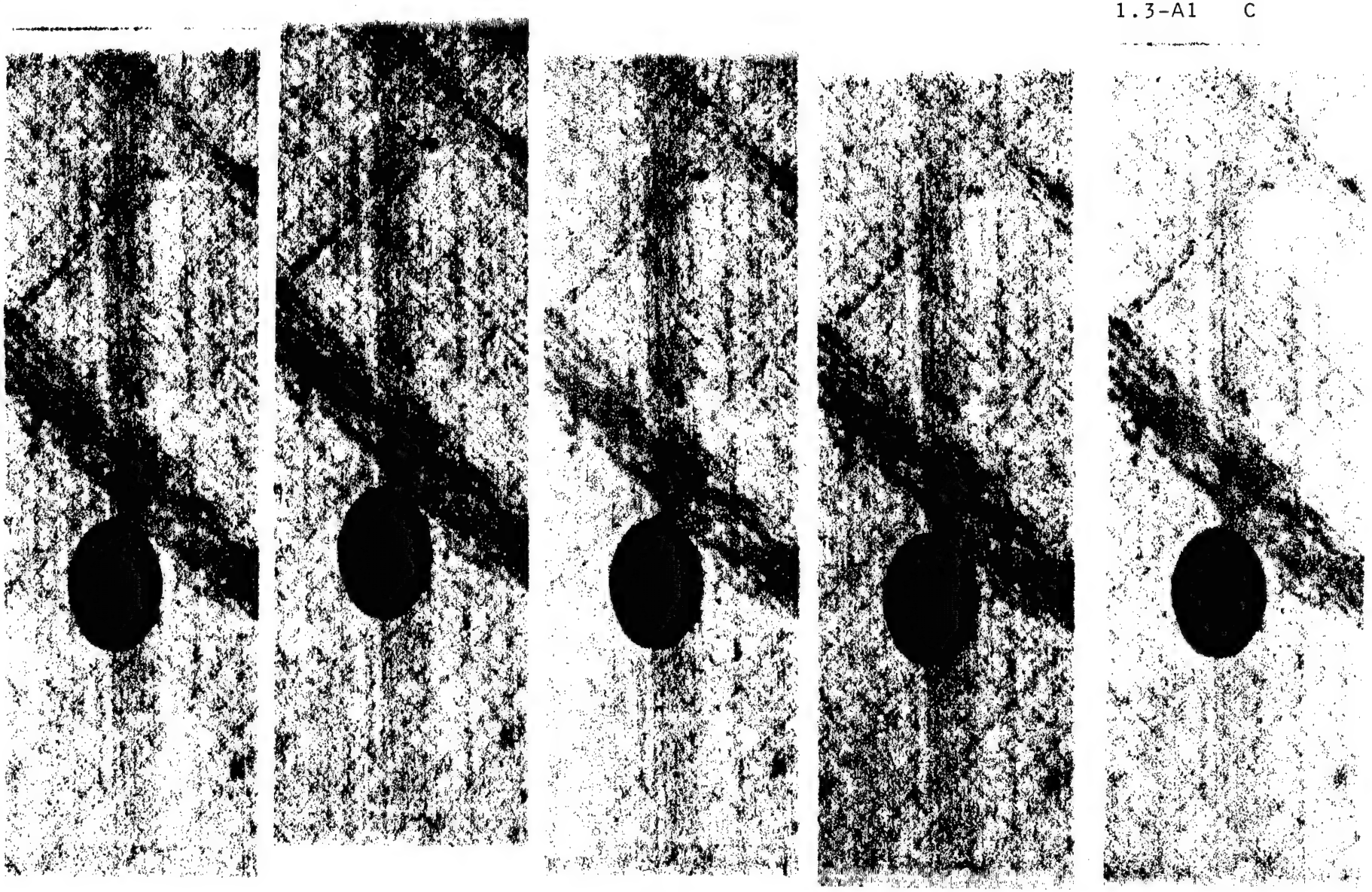

21000 26000 31000 45000 55000

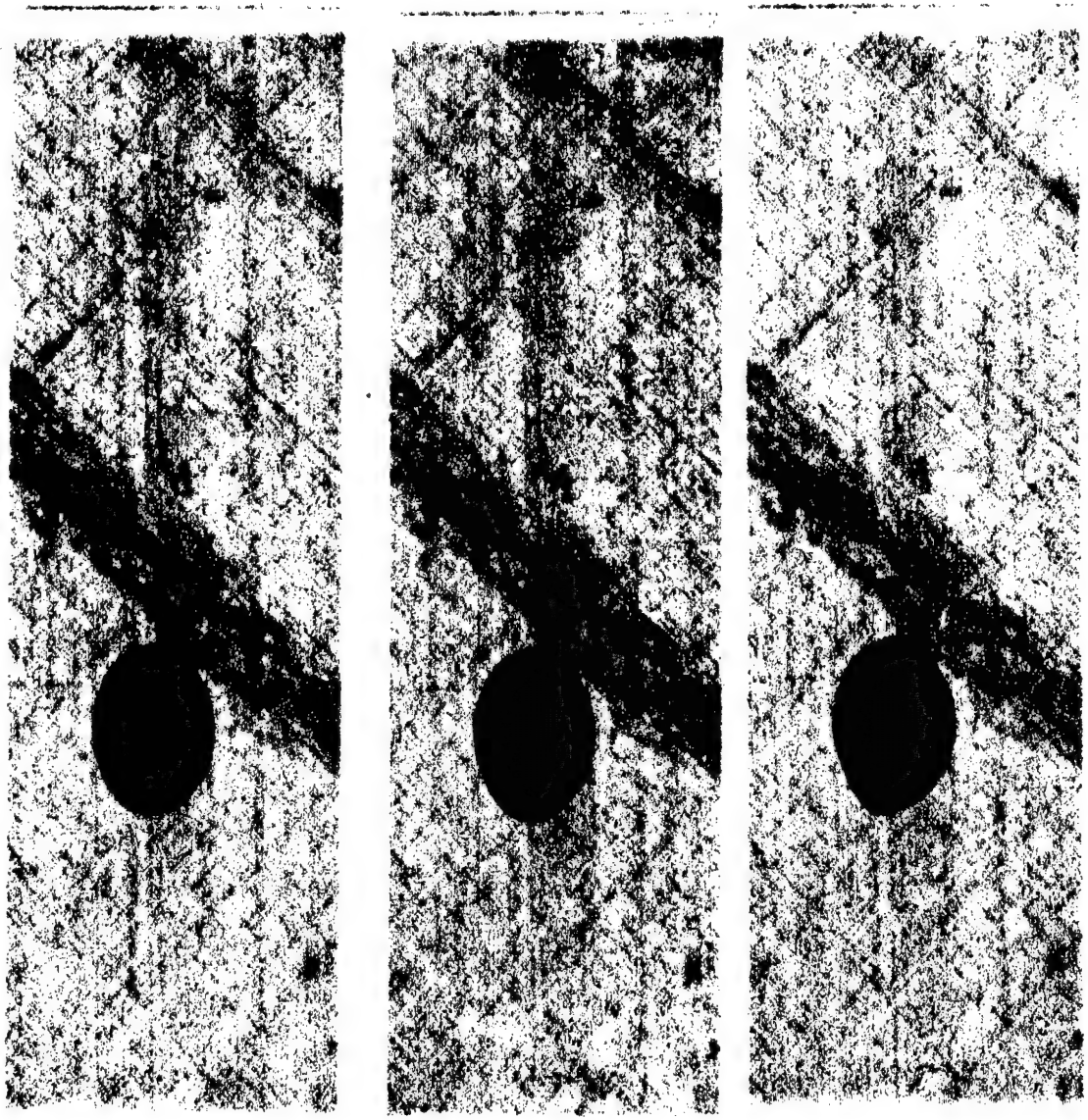

65000 85000 110,000

1.3-A1 MC

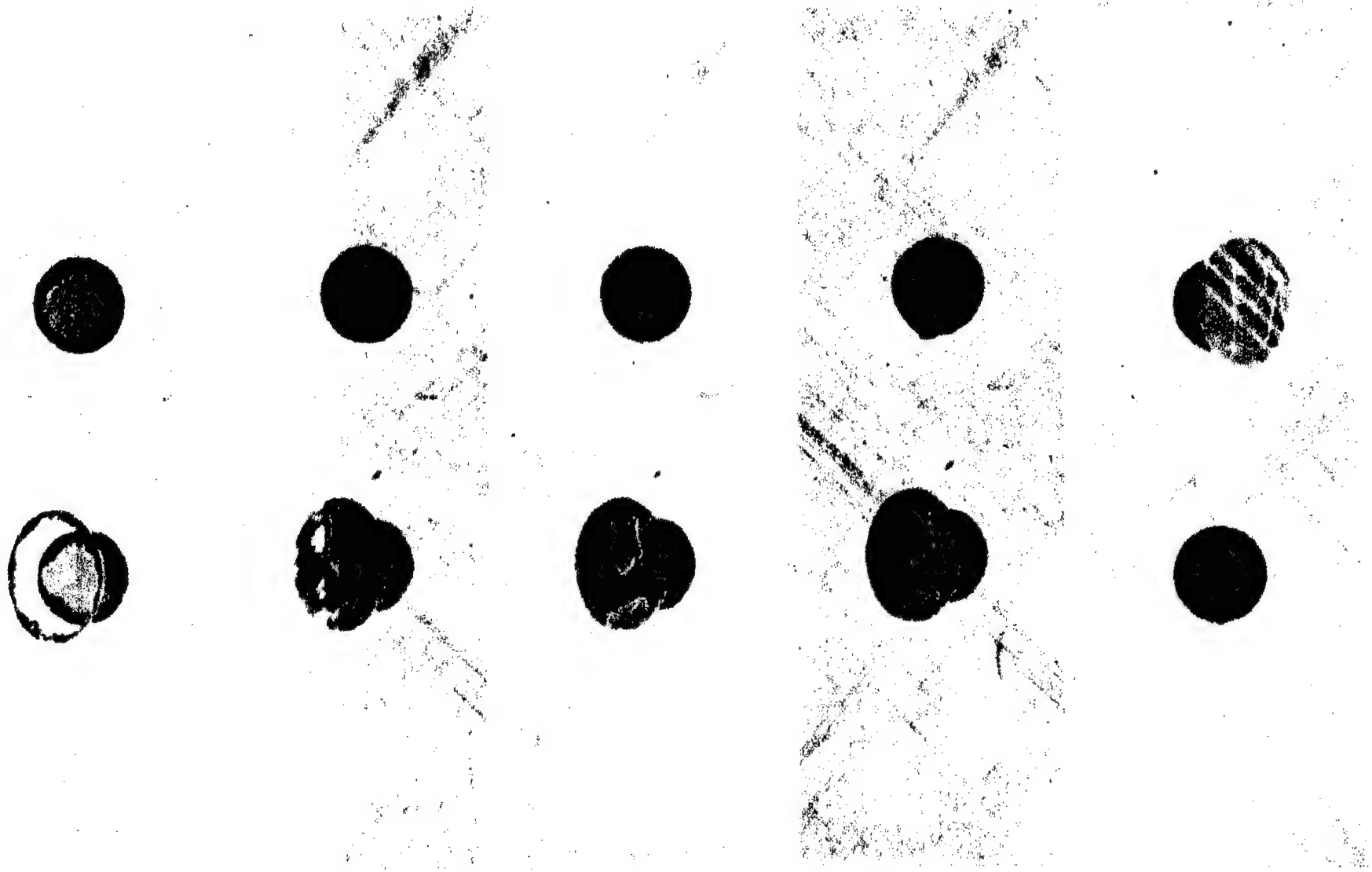

0 3000 10000 15000 18000
(MT)

1.3-A1 MC

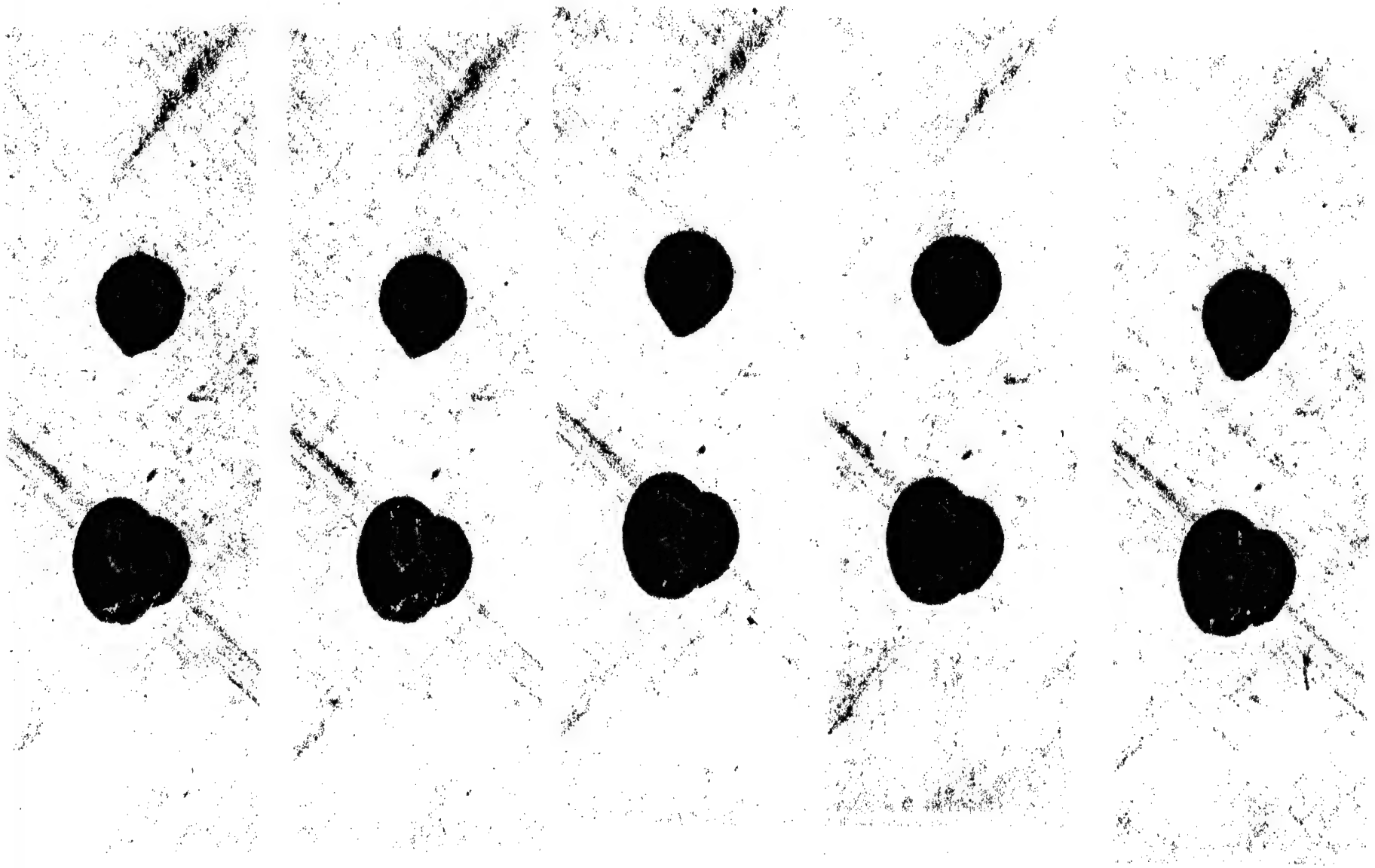

18000 21000 26000 31000 45000

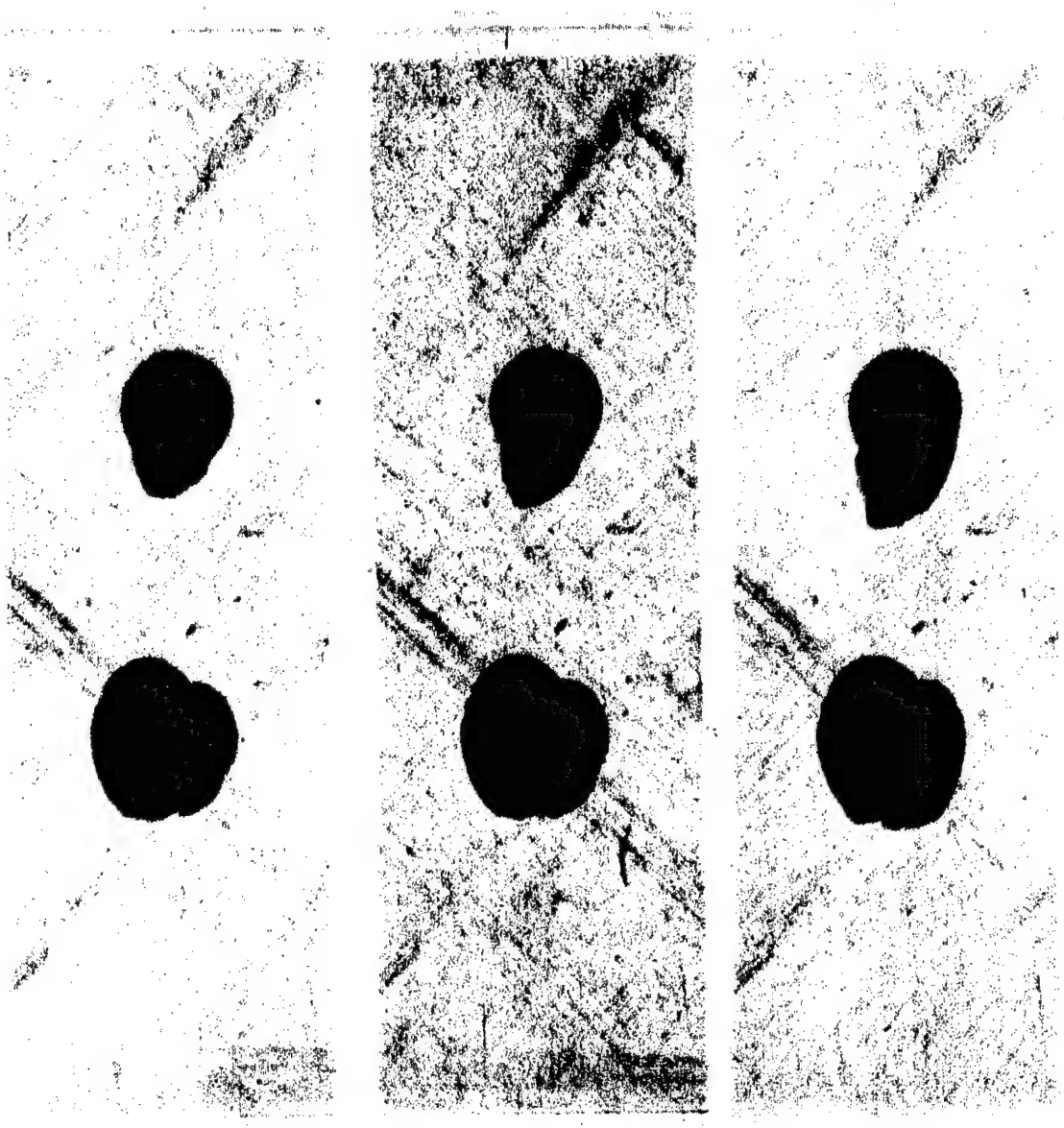

65000 85000 110,000

1.3-A1 MT

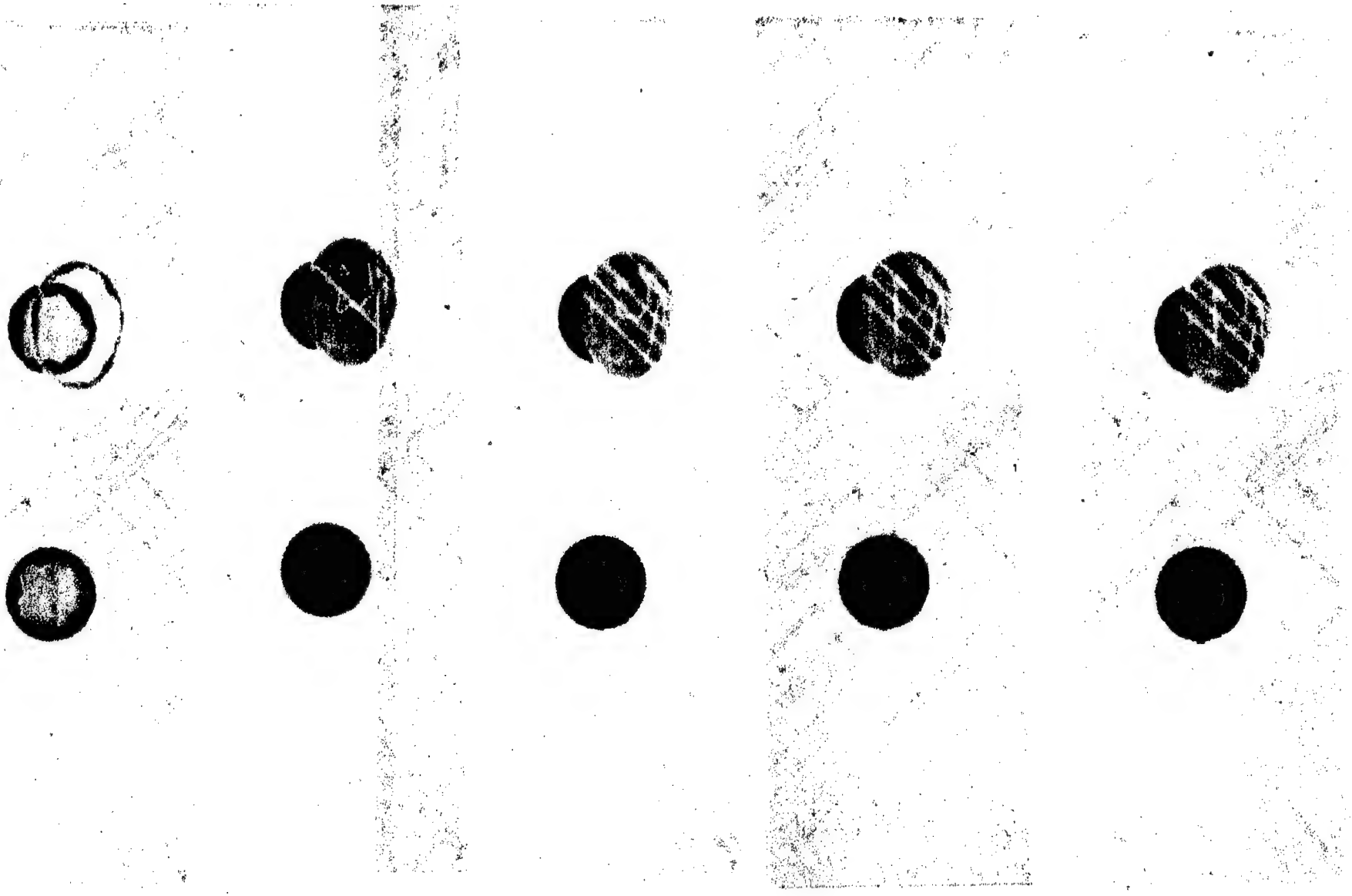

0 3000 10000 15000 18000

1.3-A1 MT

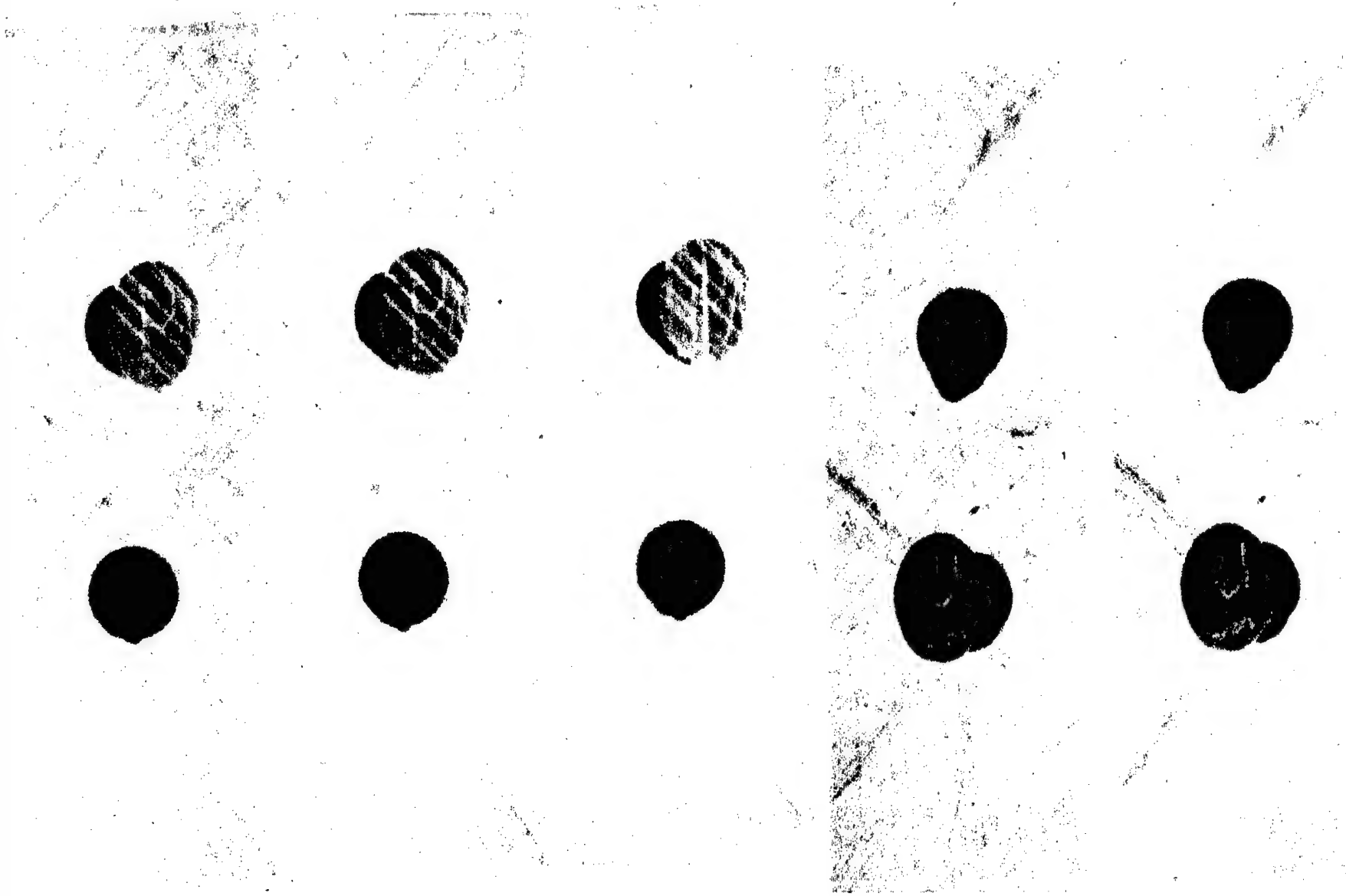

21000 26000 31000 45000 (MC) 55000 (MC)

1.3-A1 MT

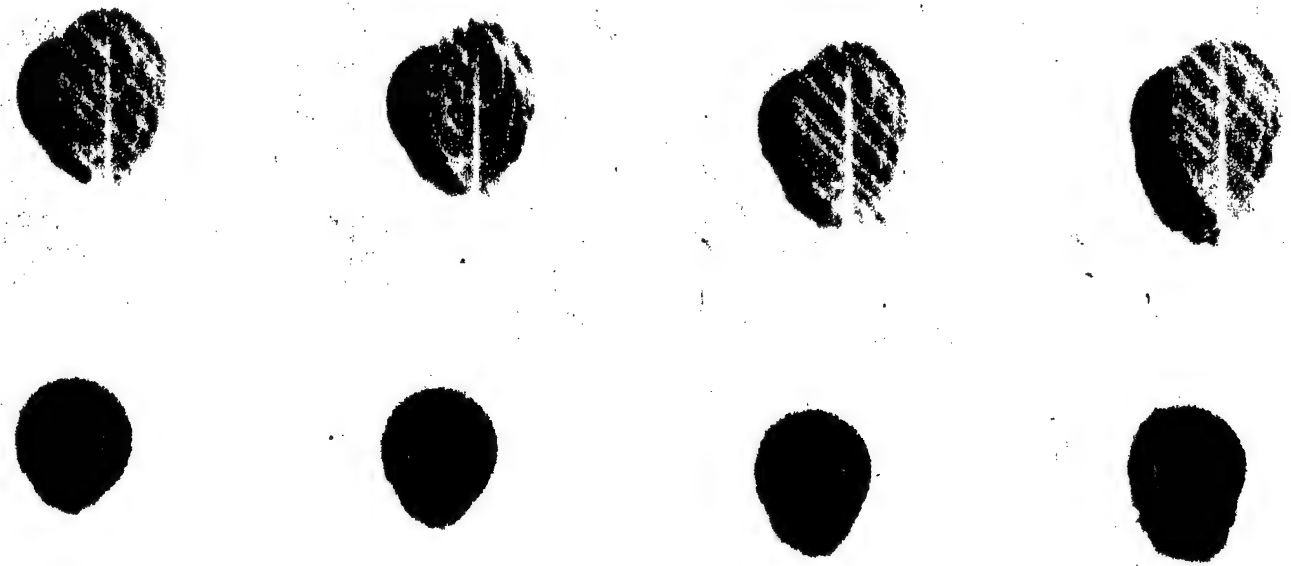

55000 65000 85000 110,000

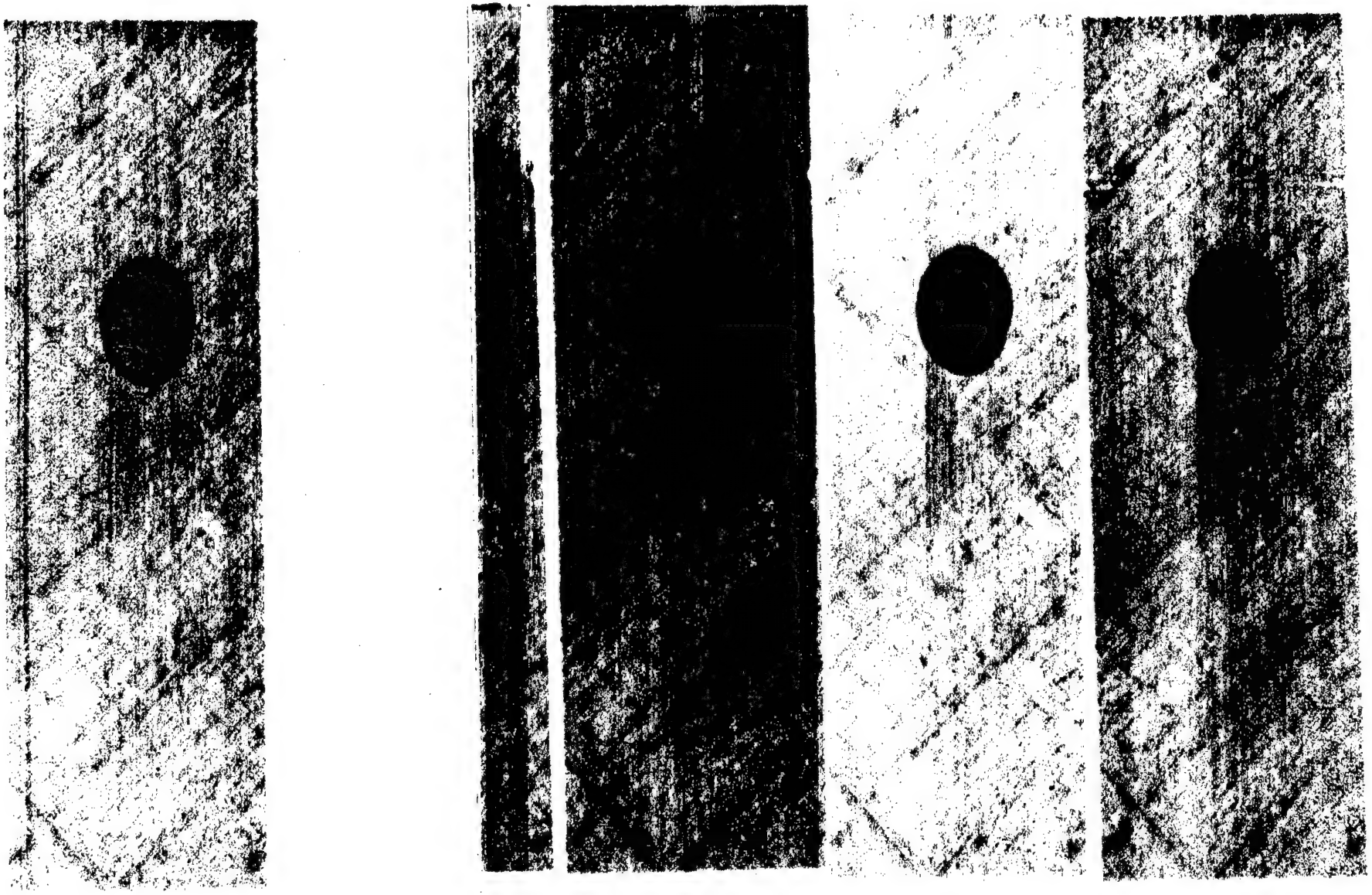

0 3000 10000 15000

1.3-A1 T

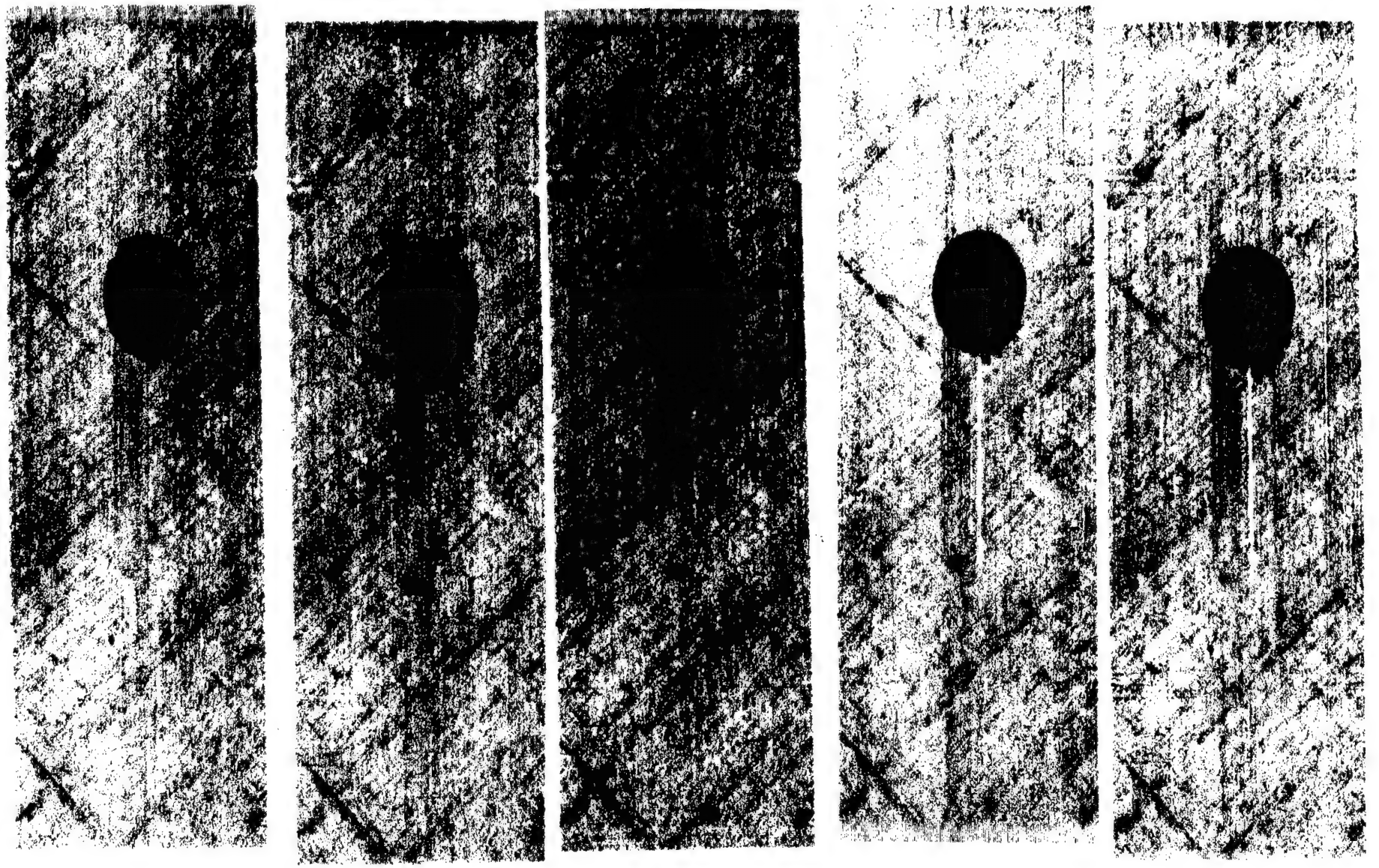

8000 21000 26000 31000 45000

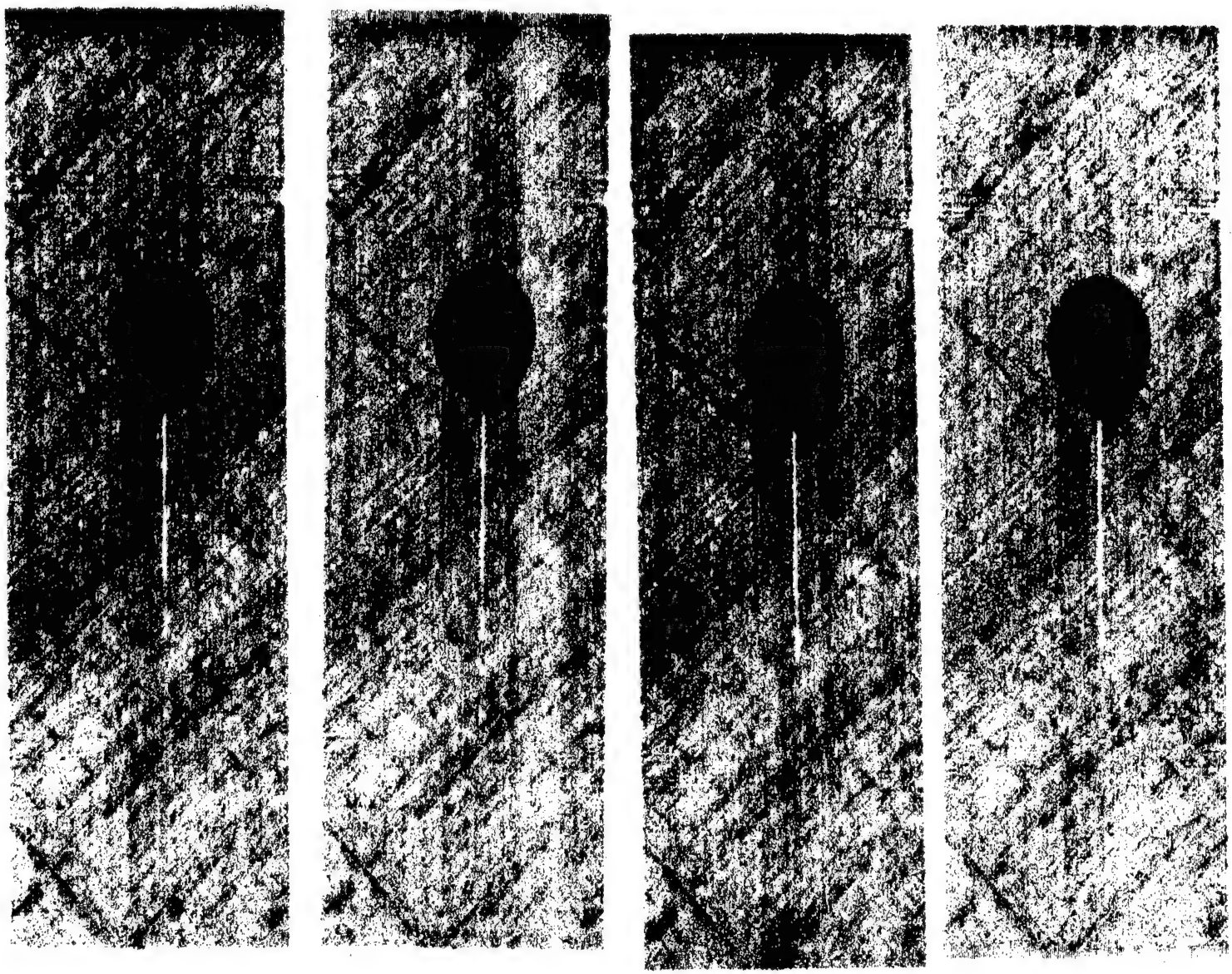

55000 65000 85000 110,000

Specimen 1.4-A3, T, C

1.4-A3 T

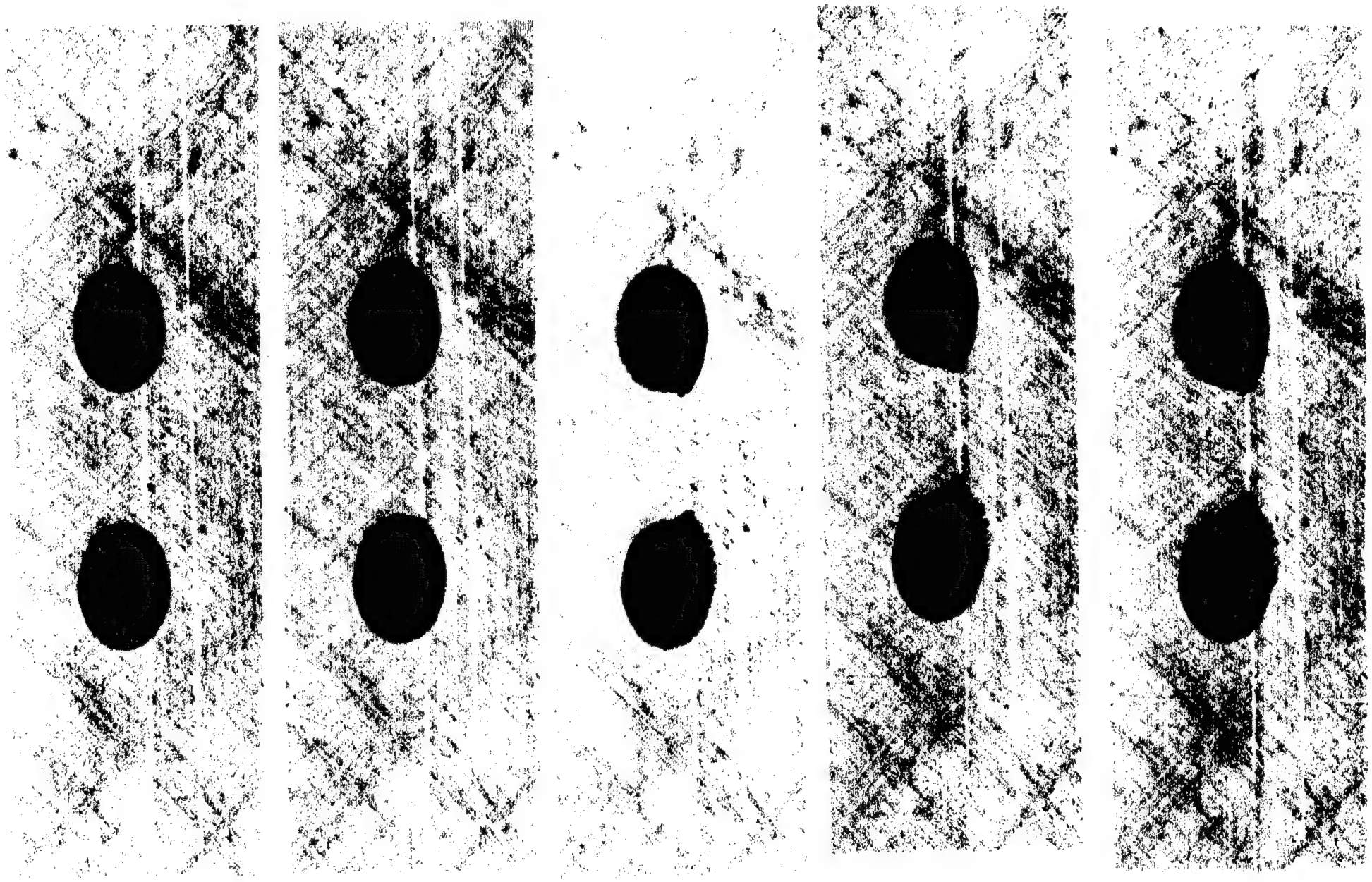

0 3000 10000 15000 18000

1.4-A3 T

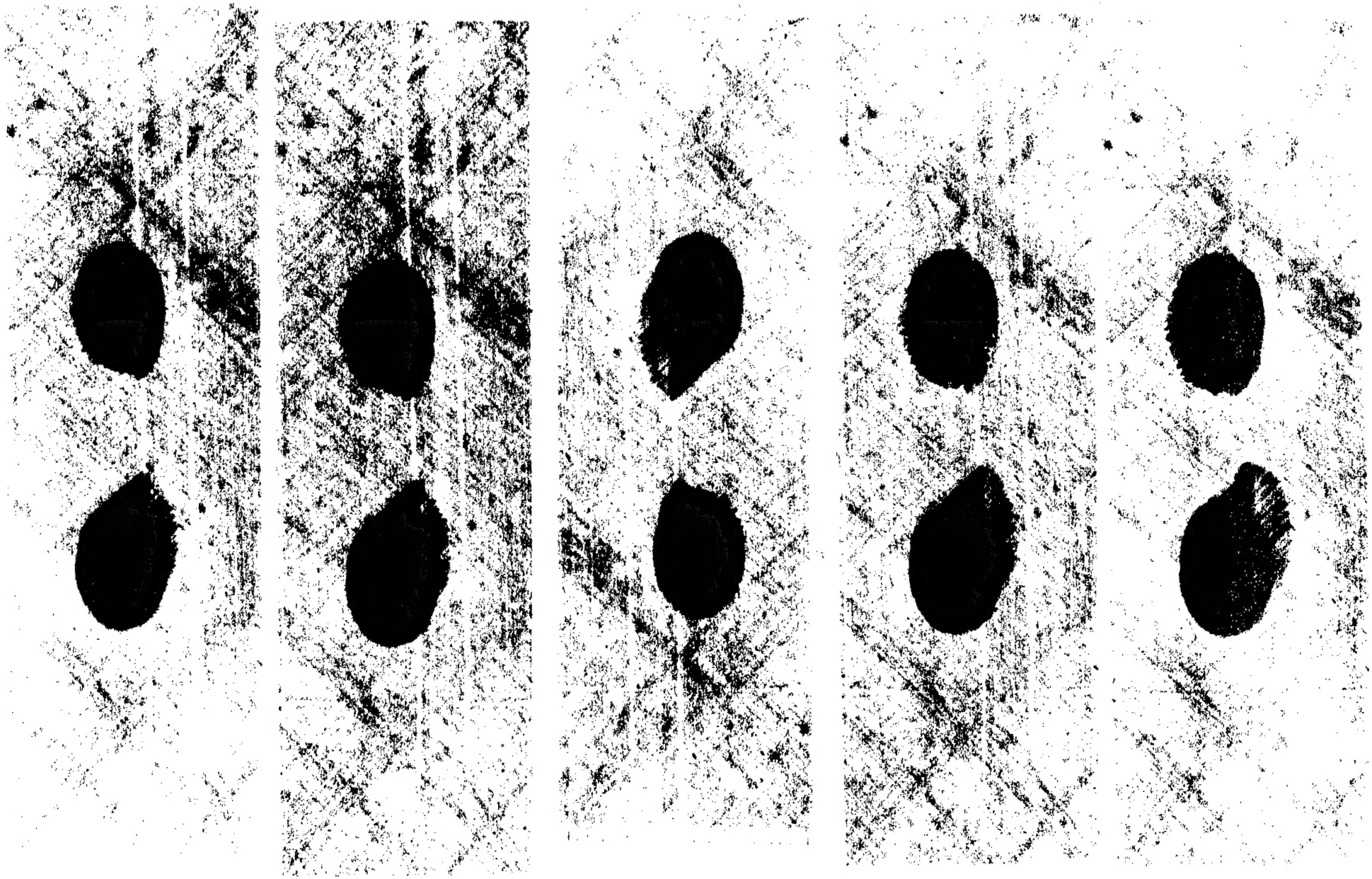

21000 26000 31000 45000 55000

1.4-A3 T

65000 85000

1.4-A3 C

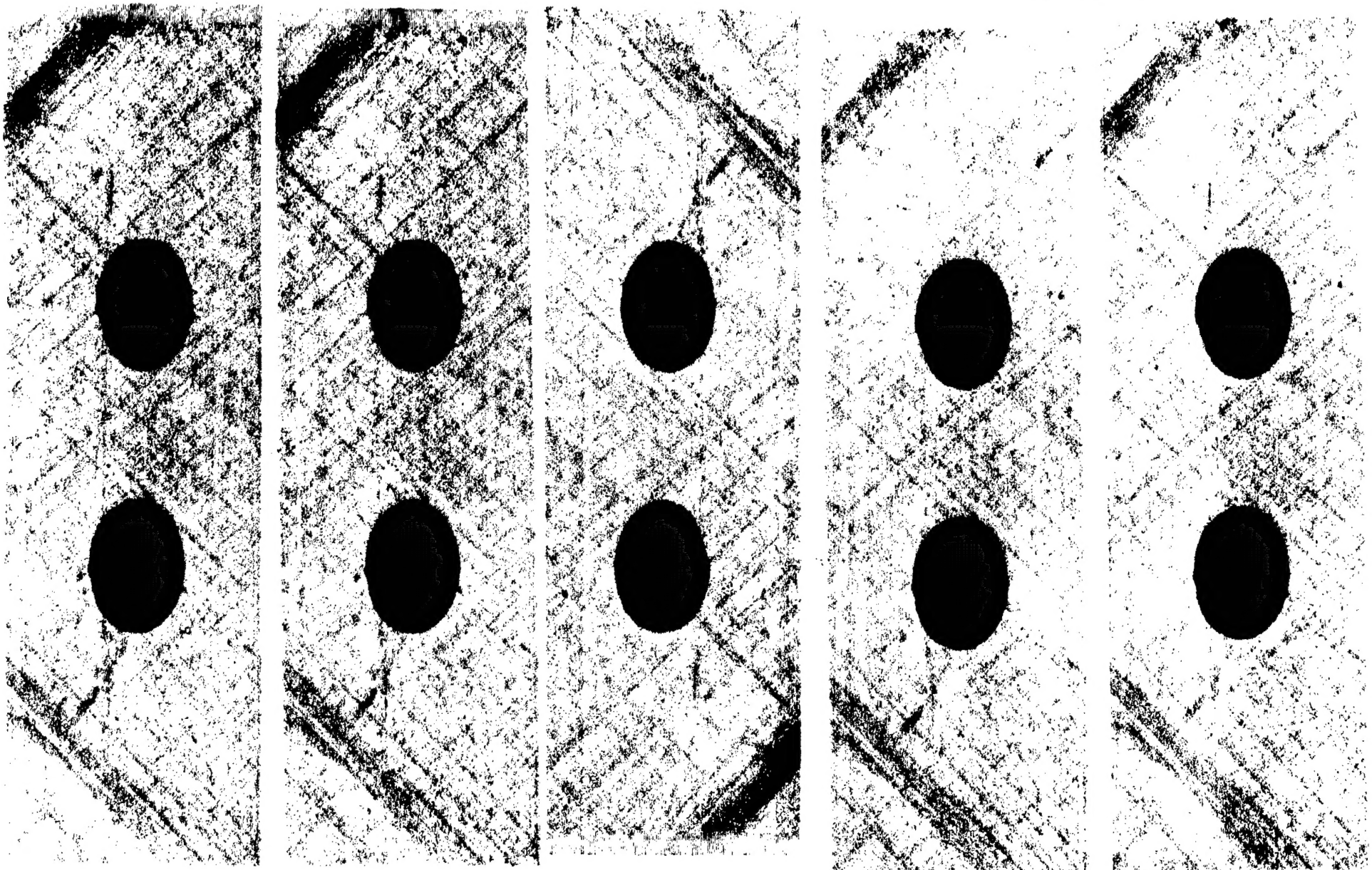

21000 26000 31000 45000 55000

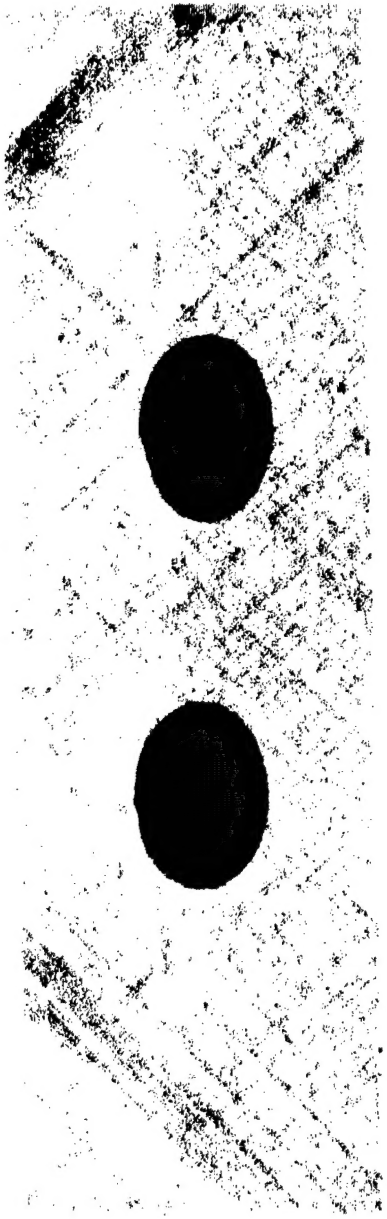

65000

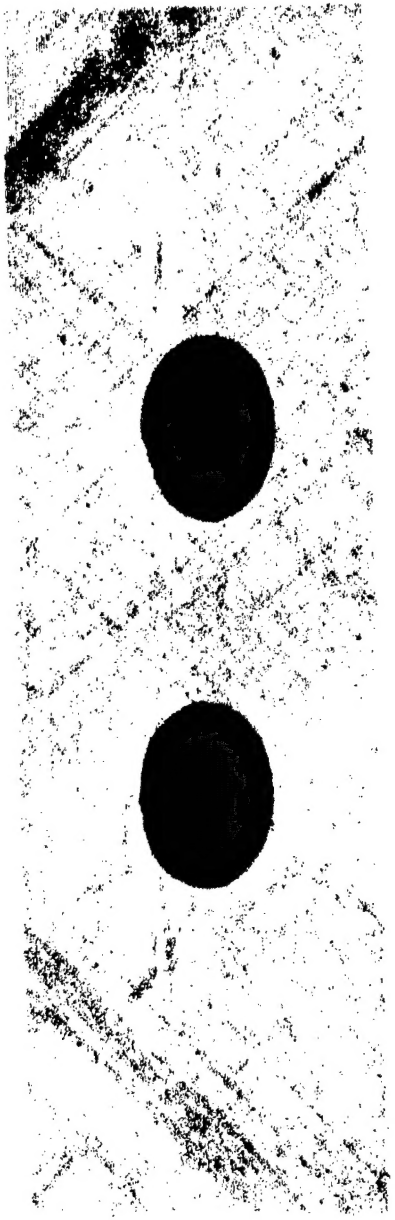

85000